Recent Advances in Hydrotropic Solvent Systems for Lignocellulosic Biomass Utilization

Soyeon Jeong,[a] Jiae Ryu,[a] Qiang Yang,[b,]* J. Y. Zhu,[c,]* Chang Geun Yoo [a,d,]*

[a] Department of Chemical Engineering, State University of New York College of Environmental Science and Forestry, Syracuse, NY 13210, USA

[b] School of Packaging, Michigan State University, East Lansing, MI 48824, USA

[c] Forest Products Laboratory, U.S. Department of Agriculture, Madison, WI 53726, USA

[d] The Michael M. Szwarc Polymer Research Institute, Syracuse, NY 13210, USA

*Corresponding authors: yangqi22@msu.edu, junyong.zhu@usda.gov, cyoo05@esf.edu

Abstract

In deconstructing lignocellulosic biomass, processing solvents directly and indirectly influence the process efficiency by reducing recalcitrance, fractionating target components, preserving/modifying biomass components, etc. Hydrotropic solvents have shown effective biomass fractionation performance due to their unique amphiphilic structure. In particular, these hydrotropes effectively separate lignin from the cellulose-rich fraction with minimum modification and maximum recovery, which aligns well with the biorefinery strategy by enhancing the recovered lignin quality and quantity. Hydrotropic solvent functions as a catalyst in biomass fractionation/degradation and also as a solvent via aggregation and clustering for the dissolution of target components such as lignin. Moreover, this solvent approach has great potential in eco-friendly manufacturing in plant biomass utilization because of aqueous processing. In this review, chemical structure, amphiphilicity, roles and mechanism of hydrotropic solvents are discussed along with their recent applications in plant biomass utilization. Current challenges in their industrial applications and perspectives on the direction of future research directions are presented.

1. Introduction

Lignocellulosic biomass is a promising resource to alternate petroleum-based feedstock because of its sustainability, renewability, and availability in large quantities in many regions of the world.[1, 2] However, its structural and compositional complexity and heterogeneity are a challenge in utilization.[3] Effective fractionation of plant cell walls into platform molecules such as cellulose-rich fraction, lignin-rich fraction, and solubilized carbohydrate fraction prior to conversion processes is beneficial for achieving maximum value in utilization.[4] The biomass processing chemicals play a vital role in reducing plant biomass recalcitrance as well as facilitating separation and recovery of the fractionated components.[5, 6] In recent years, extensive research has been conducted on biomass processing solvent systems to enhance total biomass utilization.[7-9] Biomass processing solvents including organic solvents, aqueous phase hydrotropes, and ionic liquids have been investigated to understand their effectiveness and fundamental mechanisms for biomass fractionation.[10-21] In addition to the technical performance of these solvents, their economic feasibility and environmental sustainability have been evaluated and considered in recent studies.[22, 23] Despite many efforts in studying these solvent systems, many technical barriers remained to be overcome for commercialization. For instance, many organic solvents pose fire and explosion risks due to volatile materials.[24] Many ionic liquids are toxic and difficult to synthesize and recycle.[25, 26] Among many solvents, hydrotropic solvents have also been considered as potential candidates for biomass fractionation. Ionic liquids can function as important hydrotropes. However, unlike conventional hydrotropic solvents, they are synthetic and primarily focused on improving the solubility of moderately hydrophobic compounds, such as phenolic acids from plant biomass.[27, 28] Consequently, there have been almost no prior studies that have investigated the

3

application of ionic liquids in plant biomass fractionation and conversion from hydrotropic perspective.

Hydrotropic solvents have been considered potential candidates for biomass fractionation because they are environmentally friendly and relatively safe to handle with aqueous processing, easy preparation, non-toxic, and non-volatile.[29-32] The network map with keywords in scientific publications on "hydrotropic solvent" based on the Web of Science was processed to find the hydrotrope-related subjects by the full counting method via VOSViewer.[33] As shown in **Fig. 1**, hydrotropic solvent mainly appears with its performance in aqueous phase-related words including solubilization, solid dispersion, aggregation behavior, solubility, dissolution, aqueous-solution, and water. It is also associated with biomass-related keywords such as wood, lignin, and fractionation, which are categorized into blue clusters in the network map. The hydrotropic phenomenon was first discovered in 1916.[34] Salt-based hydrotropes were studied to dissolve wood lignin for wood pulping over 80 years ago[35] and were found impractical due to very long reaction time at relatively high temperatures of approximately 150 ℃ as well as low fiber yield and inferior fiber mechanical properties.[36] Recent studies on salt-based hydrotropes expanded to biomass fractionation.[4, 37, 38]

Hydrotropes are a class of amphiphilic organic compounds that serve the purpose of enhancing the solubility of sparingly soluble organic substances in aqueous solutions.[28, 39] The amphiphilic structure of hydrotropes allows the fractionation of plant biomass through its unique interactions with both the soluble and insoluble components of biomass, dissolving the target components via aggregation with biomass fractions or self-aggregation. For instance, the hydrotropic salt-assisted lignin extraction process extracted lignin without its significant modification and cellulose.[21, 30, 32] Also, Zhu et al. at the USDA Forest Products Laboratory

discovered that hydrotropic acids, or acid hydrotropes, such as aromatic or aliphatic acids, have strong hydrotropic properties toward lignin.[21] As acids, they serve as a catalyst to hydrolyze hemicelluloses and depolymerize lignin into smaller molecules. Compared to conventional solvents and salt-based hydrotropes, acid hydrotropes do not require harsh processing conditions, such as high temperature and pressure or prolonged processing times.[40] In addition, one primary advantage of hydrotropes in biomass processing is the ease of solute recovery from the processing spent liquor via simple dilution using water, enabling the reuse of concentrated hydrotropic solvents after concentration.[21, 30, 40, 41]

This article reviews the unique properties and fundamental knowledge of hydrotropes and connects these basic understandings to recently reported technical performance in plant biomass processing. Specifically, this article introduces the fundamental understanding of the amphiphilicity of hydrotropes, their chemical structures, experimental and computational methods for the measurement, the mechanisms of hydrotropic phenomena such as clustering and aggregation, and the effects of processing conditions like size, composition, concentration, and temperature, in addition to the roles and applications of the hydrotropes in biomass processing. Fundamental knowledge about hydrotropes is vital for a deeper understanding of the reported hydrotropic effects on technical performance in plant biomass processing and facilitates further improvement and extension of their applications. A comprehensive and fundamental understanding of hydrotropes in biomass processing is also discussed, along with their current barriers to commercialization. Finally, future research perspectives are provided.
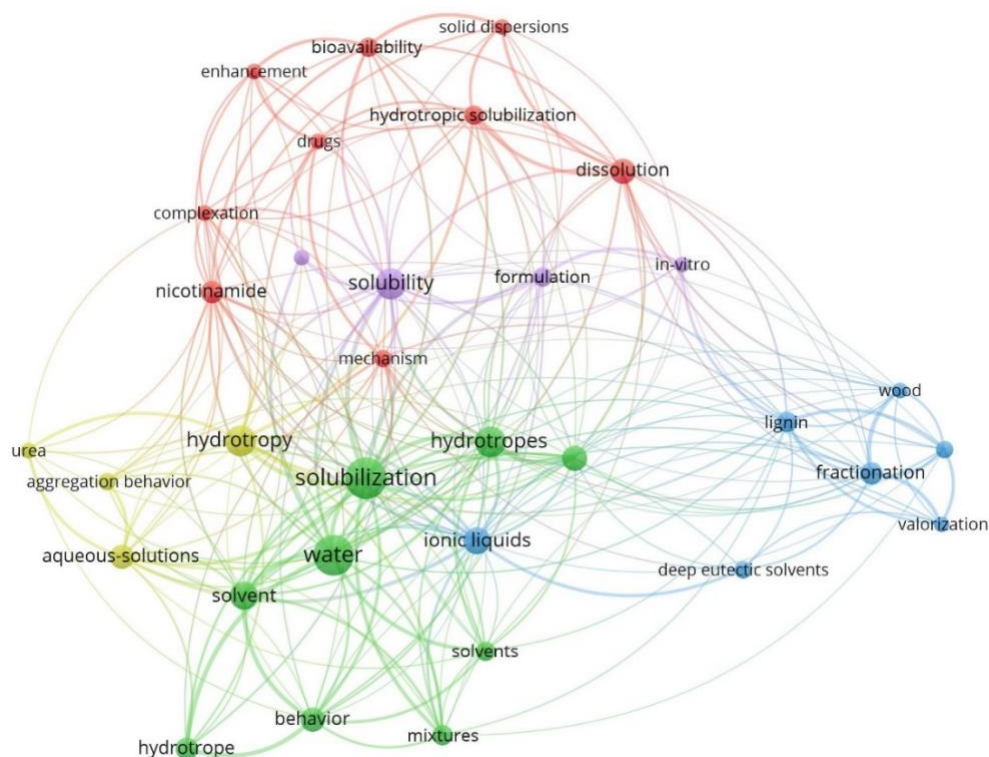
Fig. 1. The network map generated with keyword co-occurrence in scientific publications on "hydrotropic solvent" searched by Web of Science (generated August 2023).
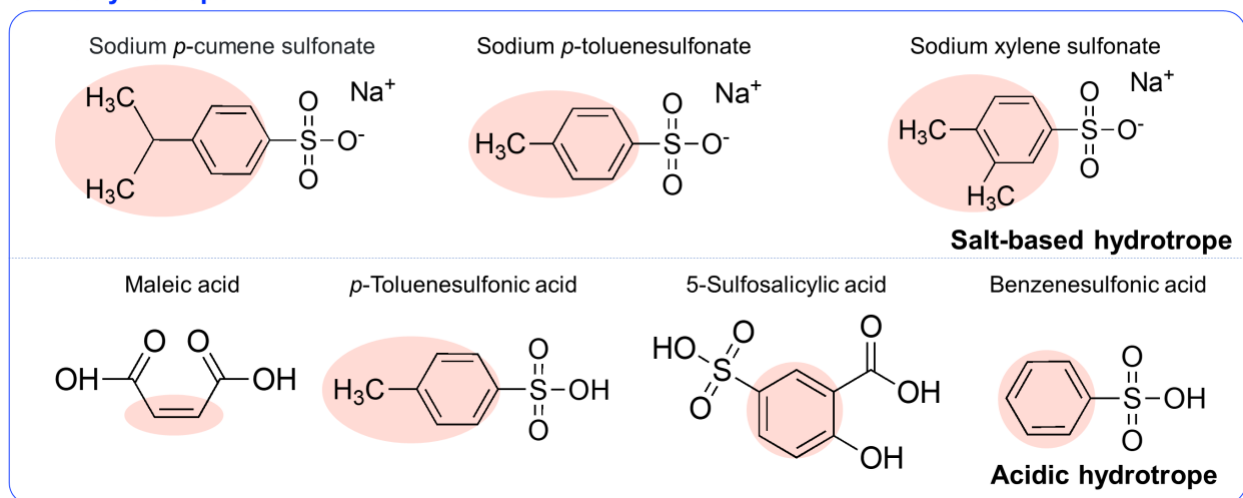
2. Characteristics of hydrotropes
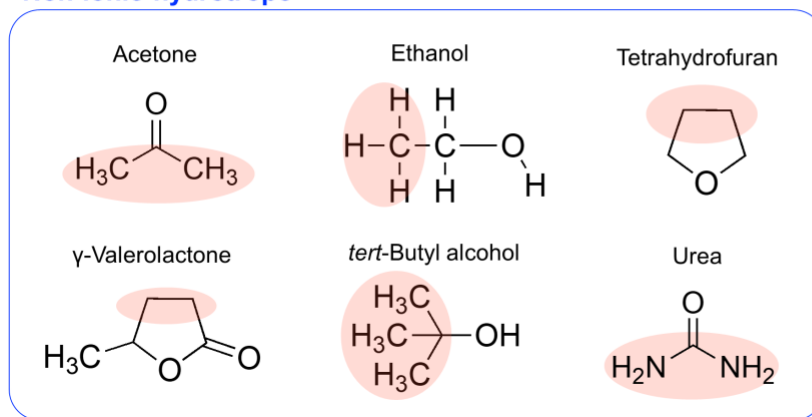
2.1 Amphiphilicity of hydrotropes

Amphiphilicity is the spatial difference between hydrophilic (polar) and hydrophobic (non-polar) regions in a molecule.[42] The amphiphilic structure of hydrotropes, composed of polar and non-polar parts together, allows them to dissolve the sparingly soluble compounds into an aqueous solution at the mesoscale.[43] Hydrotropes have been used in various applications such as solubilizing drugs, extracting chemicals for fragrances, and separating liquid from the close-boiling liquid mixture.[43, 44] Also, the efficiency of hydrotropic solubilization is important to industrial applications.[45] The hydrotropes can be classified as ionic, non-ionic, and solvo-

6

surfactant (**Fig. 2**). Salt-based hydrotropes such as sodium xylene sulfonate (SXS), sodium cumenesulfonate, and sodium benzoate,[36, 46-48] and acid hydrotropes like maleic acid,[40, 49, 50] *p*-toluenesulfonic acid (*p*-TsOH),[21, 51, 52] 5-sulfosalicylic acid (5-SSA),[4] and benzenesulfonic acid (BA).[53, 54] have been applied in plant biomass processing. As a cosolvent and conventional hydrotrope, acetone, ethanol, tetrahydrofuran, γ-valerolactone, *tert*-butanol (TBA), 2-butoxyethanol[55-58] are available. However, these solvents were not fully discussed as an aspect of the non-ionic hydrotropes in biomass fractionation because of their small size and difficulty in explaining the aggregation behavior from biomass components. Solvo-surfactant provides the behavior of surfactants and solvent together as a hydrotropic solvent such as monoalkyl glycerol ethers.[59, 60] Structurally, these solvents have an amphiphilic structure consisting of different hydrophobic and hydrophilic portions.[48, 61] For a given solute, the solubilization efficiency of the hydrotrope is dependent upon its amphiphilicity. The focus of this review is mainly on ionic hydrotropes.
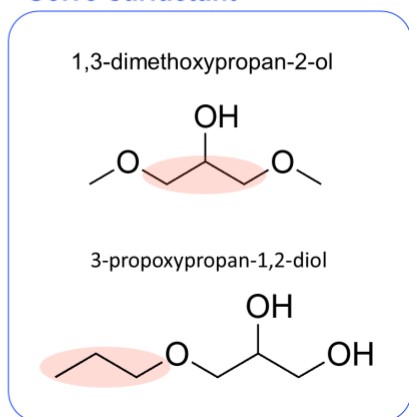
Fig. 2. Amphiphilic structure of hydrotropic solvents including ionic hydrotropes,[21, 36, 40, 46, 47, 49-52] non-ionic hydrotropes,[55-58] and solvo-surfactant.[60, 62]

Based on the bulk structure of hydrotropes, the hydrophobic moieties can be categorized into aromatic or aliphatic hydrotropes. The aromatic hydrotropes normally contain benzene, pyridine, or furan ring, while the hydrotropes have aliphatic substances such as short alkyl chains, cis-alkene, or non-polar amino acid groups, and non-polar C=C covalent bonds.[48, 49, 58-61, 63] The hydrophilic moieties of hydrotropes, such as hydroxyl and carboxyl, carbonyl, amino, and phosphate, facilitate the hydrotrope in an aqueous solution.[64] p-TsOH, having a hydrophobic component with an aromatic ring and non-polar methyl group.[65] The sulfonic acid group is the

hydrophilic component of p-TsOH and functions as an electrolyte. The sulfonic acid can be ionized or dissociated due to its electrical conductivity and dissolve biomass components in an aqueous solution.[64, 66] Maleic acid is another acid hydrotrope for plant biomass fractionation.[49] It is a dicarboxylic acid with a polar group (hydrophilic) on one side and a non-polar C=C bond on the opposite side. The experimental measurement and theoretical calculations of hydrotrope provide the behavior of the amphiphilic structure and interaction between the hydrophobic solute and hydrotropes.[32, 58, 67-70]

2.1.1 Experimental methods for amphiphilicity

The amphiphilicity of hydrotropes can be measured in binary systems such as water/oil systems with octane, cyclohexane, toluene, or n-decane as an oil phase.[71, 72] It can be quantified by ternary phase diagrams between the hydrotrope, water, and oil. The affinity of a hydrotrope to the water-rich and oil phases can be measured with the infinite dilution in equilibrium.[73] The interfacial tension disappears at a critical point because the amphiphilic structure of hydrotropes acts as a co-solvent at that point, following the decrease in the interfacial tension caused by adsorption at the oil/water interface. For example, when comparing two hydrotropes, *tert*-butanol (TBA) and 2-butoxyethanol (BEG) in a water-toluene system, TBA showed higher toluene phase separation than BEG.[74] Since the phase separation to toluene in the water-toluene system indicates the hydrophobicity of the hydrotropes, TBA has a higher hydrophobicity. The water-phase separation occurred more with BEG, indicating its relatively higher hydrophilicity. This phase diagram dictated by surface tension is also applicable to predict the amphiphilicity of hydrotropes. The surface tension of a liquid is critical when dissolving target materials. The solubilization of hydrophobic compounds such as lignin in aqueous solution by hydrotropes can be explained by

the surface tension of a liquid. The lower surface tension of the liquid can have a better lignin solubility due to the introduction of the amphiphilic structure of hydrotropes.[75]

The hydration of ions also dictates the amphiphilicity of hydrotropes.[76] Hofmeister series is the ordering of ions series, divided into two groups: strongly and weakly hydrated ions, resulting in the salting-in and salting-out behavior. (**Fig. 3**).[76, 77] The highest charge density is called kosmotropic, and the lowest one is named chaotropic. The salting-out effect is caused by dehydration by low-charged ions. Hydrotropes are hard to solubilize in an aqueous solution under this condition.[78] Using the salting-in and salting-out effects, the amphiphilic structure in a hydrotropic molecule is determined depending on its charged density from ions (**Fig. 3a**).[76] The properties related to the amphiphilicity can be observed at the lowest critical solubilization temperature (LCST), also called phase transition temperature (PTT), using a binary system such as propylene glycol propyl ether/water.[76, 79] The LCST of γ-valerolactone hydrotropes based on their concentrations and amphiphilic structures are shown in **Figs. 3b and 3c**, respectively. Dipropylene glycol propyl ether (DPnP)/water (55/45, wt/wt) mixtures with different concentrations of amphiphilic molecules in the previous study showed the salt-out effect of sodium benzyl phosphate (SBP) and sodium benzyl phosphonate (SBPho), indicating that the surface tensions of those two molecules are the highest among the hydrotropes.[80]
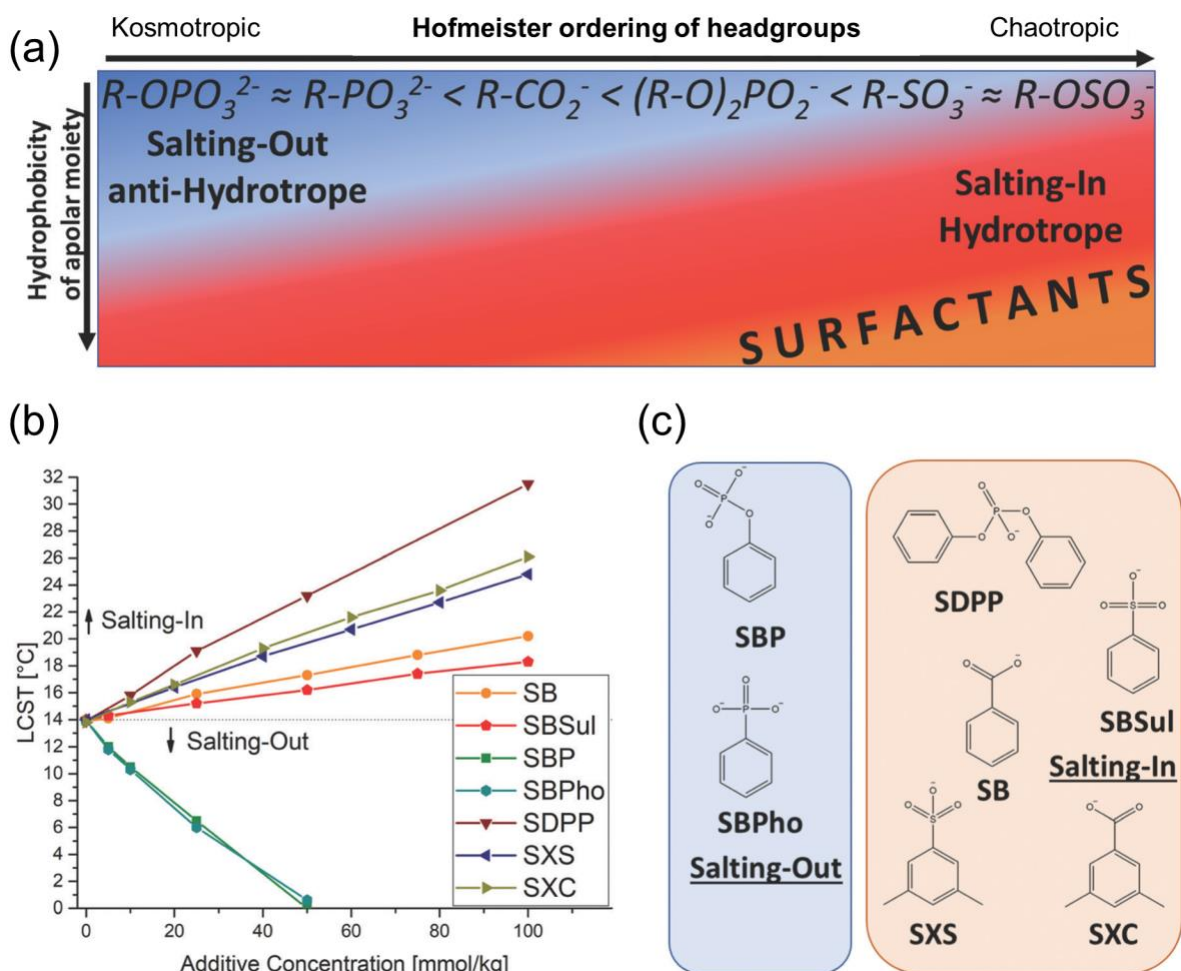
Fig. 3. Salting-in and salting-out effect on hydrotropes (a) overall impact of hydrophilic-charged group and hydrophobicity, (b) lowest critical solubilization temperature (LCST) of amphiphilic molecules (c) chemical structure; blue box: sodium benzyl phosphate (SBP) and sodium benzyl phosphonate (SBPho) and red box: sodium diphenyl phosphate (SDPP), sodium benzoate (SB), sodium benzyl sulfonate (SBSul), sodium xylene sulfonate (SXS) and sodium xylene carboxylate (SXC). Reproduced with permission.[76]

2.1.2 Theoretical calculations for amphiphilicity

The amphiphilicity of hydrotropic structure generates an asymmetric distribution of electron density. The positive charge would be formed in a molecule when the electronegative atoms move the electron density away from the sigma (σ) profile region. The sigma profile (e/Å^2), also known as sigma-hole and surface polarization charge density, can be calculated by the conductor-like screening model for realistic solvation (COSMO-RS). The sigma (σ) profile can be divided into three parts, based on the cut-off values of hydrogen bonding: hydrogen bonding donor under -0.0082 e/Å^2, hydrogen bonding acceptor over 0.0082 e/Å^2, and the non-polar region between them (**Fig. 4**). The polar properties of hydrotropes can be understood by the σ profile. For example, the symmetric carbon chain and carboxylic acid group of lauric acid represented its non-polar region (green color, **Fig. 4**) and hydrogen bonding region (red and blue colors, **Fig. 4**), respectively, based on its σ-profile.[81] Similarly, the sigma profile of sodium benzoate demonstrated the aromatic ring as a non-polar region and the sodium acetate group as a polar region. Mehringer et al. compared sodium trichloroacetate and sodium acetate by COSMO-RS calculations.[76] The authors reported that redistribution of trichloroacetic decreased the hydrated ions because of the low charge density of the hydrotrope. The aromatic ring also affected the hydrophobicity of hydrotropes because its electronegative carbon draws electron density from opposite parts such as carboxylate in cyclohexyl carboxylate.[76, 81] The effects of the hydrogen bond region of hydrotropes obtained by the sigma surface and sigma profile on plant biomass processing have not been fully discussed yet.
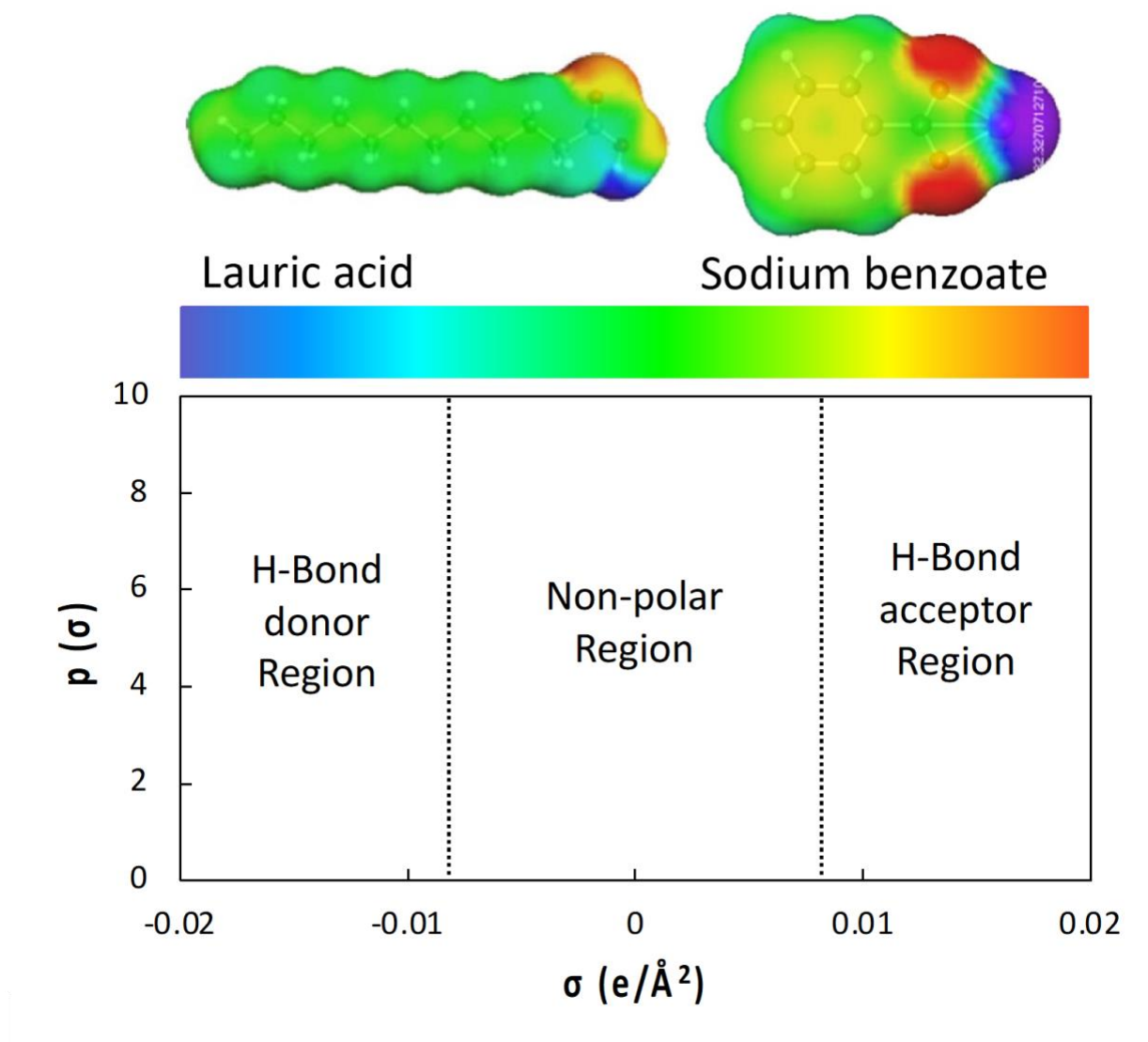
Fig. 4. Sigma surface and electroactive region of sigma profile of hydrotrope calculated by COSMO-RS methods. The sigma surface of lauric acid and sodium benzoate are adopted with permission.[81]

The amphiphilicity of hydrotropes can be predicted by log P using its sigma profiles, where P is the octanol-water partition coefficient that indicates the difference in solubility between the two immiscible solvents. The log P can be estimated by free energies, but experimentally

measuring solvation-free energies is challenging.[82] Molecular dynamic simulations are often used instead. The concept of log P is derived from the octanol-water partition coefficient of lipophobic (hydrophilic) and lipophilic (hydrophobic) structures. A lipophilic structure, which is used interchangeably with a hydrophobic structure, is attracted to oil, lipid, and non-polar solvents.[83] It can be accepted to the oil phase and has a high log P value.[84] On the other hand, the hydrophilic (lipophobic) hydrotrope presents a lower value of log P.[85] As a result, log P indicates the hydrophobicity and hydrophilicity of the hydrotropes. The ChemDraw calculated log P values of acid hydrotropes applied in the biomass processing are shown in **Fig. 5.** The lower log P value is favorable with the aqueous phase. BA presents a lower log P (1.19) than *p*-TsOH (1.68), because the methyl group on *p*-TsOH provided more hydrophobicity. The log P value of maleic acid (-0.36) indicates its relatively high hydrophilicity among the acidic hydrotropes, as shown in **Fig. 5**. The log P can be changed depending on the pH condition. The log P of 4-Cl-BSA was from –0.5 to – 0.6, depending on the pH level 0 to 2.[86] The results indicate that the hydrophilicity of the hydrotrope increased by the ionization generating sulfonic acid group as pH increased.
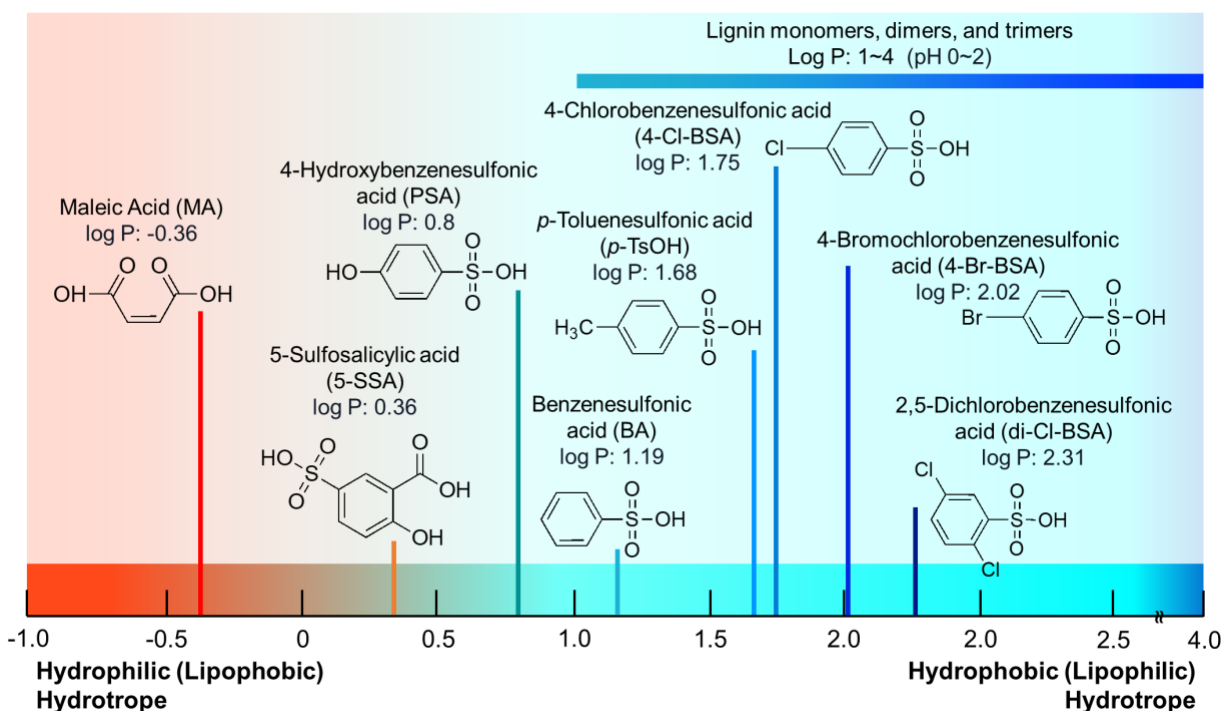
Fig. 5. Log P values of acidic hydrotropes in biomass processing and their chemical structures.

2.2. Clustering and aggregation behaviors

Hydrotropes have a markable ability to improve the solubility of generally insoluble hydrophobic substances in an aqueous medium because they possess an amphiphilic structure.[87] It is generally believed that clustering and aggregation behaviors of hydrotrope prior to or upon the addition of hydrophobic solute dictate the interaction and subsequent hydrotropic solubilization of hydrophobic lignin and extractives.[30, 88, 89] The size of hydrotropes and composition, concentration, and temperature of hydrotropic solution determine the clustering and aggregation behaviors.[90]

2.2.1 Effects of size and composition of hydrotrope on its self-aggregation

15

Some hydrotropes have too small hydrophobic moieties to self-aggregate unless a hydrophobic solute is added. Upon the addition of a poorly soluble hydrophobic solute, a very weak pre-structure with a highly dynamic, loose hydrogen bonding network between the hydrotrope and water can be established to form hydrotrope-rich and water-rich domains in equilibrium.[91, 92] It can be verified through molecular dynamics simulation, small-angle neutron scattering (SANS) and dynamic light scattering (DLS) experiments. The established bicontinuous pre-structure of hydrotrope in water is presumably attributed to the subsequent mesoscale solubilization of hydrophobic solute. Mechanistically, hydrotrope can solubilize hydrophobic solute through the hydrotrope-rich bulk phase and/or within the interfacial area in such a bicontinuous system with hydrotrope-rich domain, water-rich domain and interface. For a given hydrotrope, the solubilization mechanism is barely decided by the hydrophobicity of solute in water. Instead, the solubilization of a hydrophobic solute can be explained by two mechanisms: (i) pseudo-bulk solubilization of hydrophobic compounds within the aliphatic-rich part of pre-structured hydrotrope-water mixture and (ii) interface solubilization of hydrophobic compounds, which are still slightly amphiphilic, within the interfacial film.[91] The solubilization power of hydrotrope is thus dependent upon both the formation and extension of the pre-structure of hydrotrope in water and the hydrophobicity of the solute. However, the hydrophobic tail in hydrotropes is usually too small to cause spontaneous self-aggregation when the carbon number of the alkyl chain is under 4.[58] Abranches et al. evaluated the performance of hydrotrope depending on the different apolar volumes of alkanediols (1,2-alkanediols and 1,n-alkanediols) to enhance the solubility of syringic acid into aqueous solution.[93] The smaller 1,2-alkanediols showed a higher solubilization performance even if the self-aggregation is more favorable in the large one, which implies that the stabilization of the self-aggregated cluster in aqueous solution is also crucial as

16

solubility enhancers.[93] For these reasons, short-chained (small) hydrotropes are more favorable for hydrophobic solutes bearing polar hydroxyl and carboxylic acid functional groups such as lignin. Currently, acetone, ethanol, tetrahydrofuran, and γ-valerolactone are the most commonly used small aliphatic hydrotropic solvents in biorefinery for solubilizing lignin fragments.[55-57]

The ratio of hydrophilic and hydrophobic parts of the hydrotrope is important for self-aggregation.[85] Aromatic hydrotropes are assumed to stepwise self-aggregate to form non-micelle and stack-type aggregates or clusters in an aqueous medium, which enables the hydrotrope to solubilize the hydrophobic solutes in water.[48, 94] A larger hydrophobic part of the hydrotrope provides a better hydrotropic solubilization efficiency.[58] A hydrophobic substituent can increase the overall hydrophobicity of the hydrotrope, enhancing the hydrotropic solubilization performance.[95] A substituent is also able to introduce steric repulsion force, depending on the size and configuration, which affects the aromatic attractive interaction and hydrotropic solubilization efficiency. However, an aromatic hydrotrope should have high water solubility while maintaining hydrophobicity. If it is too hydrophobic, the solubility of aromatic hydrotrope in water is limited. Compared to aliphatic hydrotropes, aromatic hydrotropes were able to interact with lignin fragments more effectively through pronounced aromatic attractive interactions. On the other hand, the charge nature and strength of the hydrophilic part were less significant to the solubilization efficiency of aromatic hydrotropes.[45]

2.2.2. Effects of concentration and temperature

The self-aggregation of hydrotrope depends on the proportions of water, hydrotrope, and solute (**Fig. 6**). The self-aggregation tendency of hydrotropes is exothermic, contributing to their ability to solubilize compounds.[90] The hydrophobic interaction occurs between the hydrotropic

solvent and solute during the formation of self-aggregation and clustering.[96, 97] This interaction can be a hydrophobic association including π-interactions. The minimal hydrotrope concentration (MHC), representing the minimum required hydrotrope concentration in the aqueous phase, acts as a critical threshold for hydrotrope molecules to initiate aggregation.[58, 98] One potential method for improving solubility is the hydrotrope's self-aggregation process, which results in clusters surrounding the solute molecule at the MHC.[90] When the concentration of hydrotropes exceeds the MHC, they can gradually self-assemble into non-micellar and stack-type aggregates or clusters.[99] These aggregates offer a microenvironment with lower polarity and increasing microviscosity, enabling them to form complexes with hydrophobic solutes through hydrophobic interactions.[48] This "mesoscopic droplet" phenomenon allows hydrotropes to solubilize hydrophobic solutes in water for both ionic and non-ionic hydrotropes.[48] Above the MHC, the solubility of the solutes in an aqueous phase increases significantly. The solubility of solutes increases until a specific concentration of hydrotrope is reached, beyond which no significant increase in solute solubility is observed in the aqueous phase.[98] This concentration of hydrotrope in the aqueous phase is referred to as the maximum hydrotrope concentration (C_{max}).[98] Above the C_{max} point, there is no noticeable increase in the solubility of solute.[100] Also, the mesoscale inhomogeneities (aggregates or droplets) can be formed with two distinct pseudo phases (aqueous-rich and organic-rich) in the nano range, which happens in a pre-Ouzo region. This effect is observed in non-ionic hydrotropes, especially co-solvents such as ethanol, *tert*-butanol, and acetone.[101-104] The stability of the pre-Ouzo effect is determined by the size distribution of aggregates, and this effect is close to the phase separation.[104, 105]

MHC and C_{max} values are critical because of the efficient recovery and reuse of hydrotropes in industrial settings.[44, 106] Hydrotropes can solubilize more hydrophobic solutes, although they

have a lower hydrophobic component than general surfactants.[107] Unlike surfactants that form well-organized spherical micelles, hydrotropes do not undergo micelle formation and demonstrate weaker hydrophobic effects, primarily due to their shorter and/or branched alkyl chains.[44] Consequently, hydrotropes require a higher MHC compared to surfactants owing to their shorter and smaller size.[90] Both the hydrotrope itself and the solute influence the MHC and C_{max} of hydrotropes, which are useful in predicting the recovery.[44, 106, 108, 109] Therefore, the MHC and C_{max} are worth considering with lignin solubilization together to achieve the economic feasibility of hydrotropic systems in biomass processing.
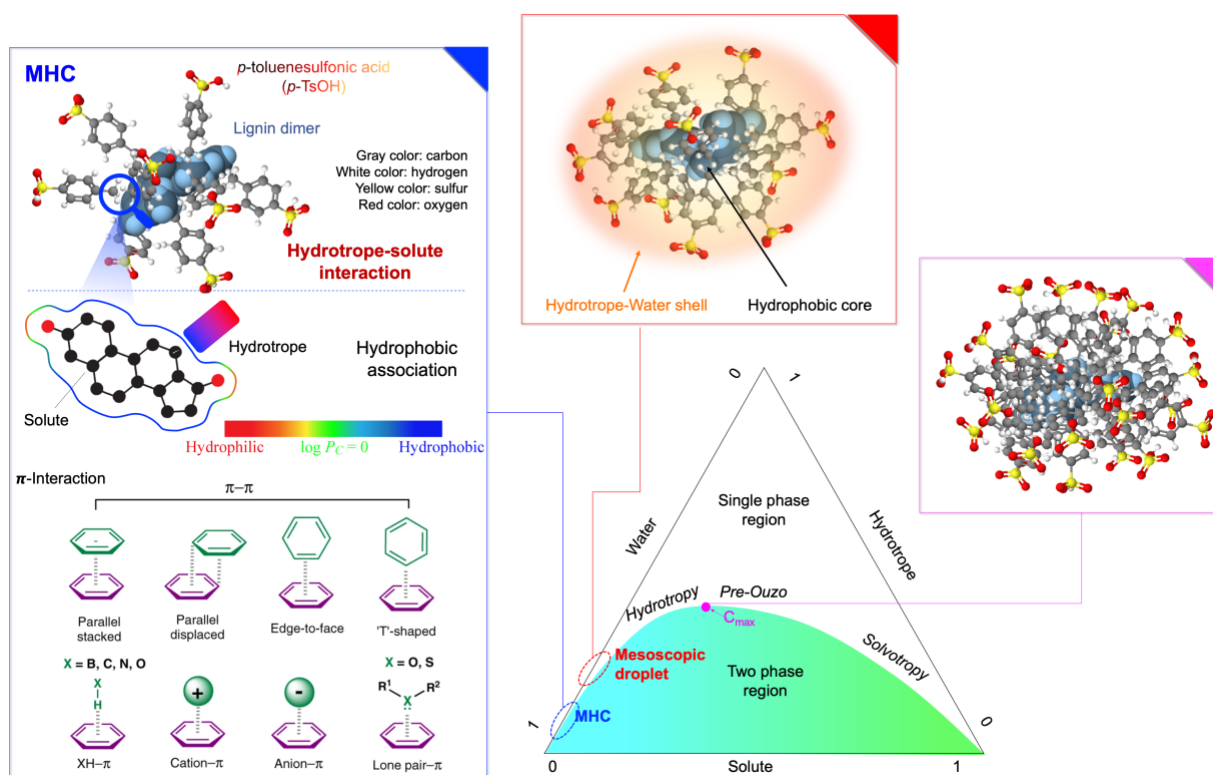

Fig. 6. Mechanism of hydrotropes aggregation phenomenon with the proportions of water, solute, and hydrotrope. (Redrawn from references.[92, 96, 97, 104]; The 3D structures of lignin dimer and *p*-TsOH were drawn using Molview software.)

Studying the dilute hydrotrope region is crucial for the economical use of smaller hydrotrope quantities and a better understanding of the molecular mechanism underlying hydrotropes.[60] The temperature of the hydrotropic solution is critical to the MHC and C_{max}. The Setschenow constant (K_s) represents the effectiveness of a hydrotrope under specific conditions of concentration and temperature.[44, 106] A higher K_s indicates that the hydrotrope is more effective at enhancing the solubility of the solute in the solution, suggesting a greater preference for solute-hydrotrope interactions over solute-water interactions.[60] The K_s is obtained by analyzing experimental solubility data and calculated using the equation $\log[S/S_m] = K_s[C_s - C_m]$, where S and S_m represent solubilities at any hydrotrope concentration (C_s) and minimum hydrotrope concentration (MHC or C_m), respectively.[110] Comparing K_s values for different hydrotropes and solutes at various temperatures allows the determination of their effectiveness order.[100]

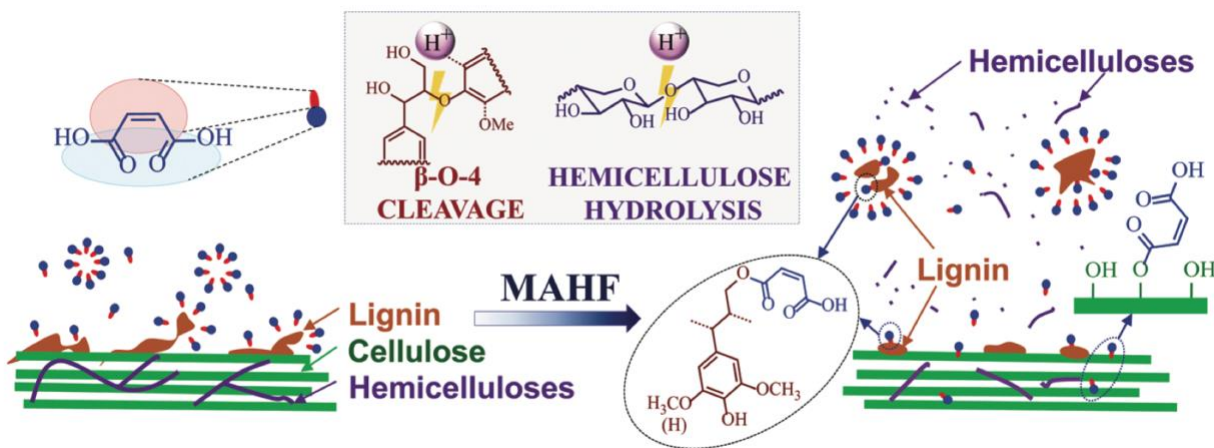## 3. Roles of hydrotropes in biomass processing

Fig. 7. Roles of maleic acid hydrotrope in biomass processing as a solvent, catalyst, and functionalizing agent, adopted with permission.[49]

3.1 As a catalyst

Investigating the correlation between acidity and the structural properties of hydrotropes is crucial in enhancing the efficiency of hydrotropic solvents in lignin and hemicellulose separation from plant biomass. Understanding the acid characteristics of hydrotropes needs both theoretical calculations and practical measurements of acidity. Theoretical calculations provide insights into the inherent acidity based on molecular structure, while experimental measurements offer direct observations of the acid behavior in the solution. Furthermore, these methods assist researchers in evaluating and comparing the acidity of various compounds and their influence on various processes, such as lignin fractionation in the study mentioned previously.[86, 111] He et al. presented a comprehensive study on the theoretical calculation and experimental measurement of acidity for catalytic hydrotropic acids.[86] Specifically, they focused on the comparison of acidity between hydrotropic acids, including 4-Cl-BSA, benzenesulfonic acid (BSA), phenol-4-sulfonic acid (PSA or 4-OH-BSA), *p*-TsOH, 2,5-dichlorobenzenesulfonic acid (di-Cl-BSA), and bromobenzenesulfonic acid (4-Br-BSA) by the proton concentration.

The pKa represents the pH at which approximately half of the acid molecules dissociated into their corresponding conjugate base forms. The calculated pKa values were utilized to compare the relative acidity among various hydrotropic acids, including 4-Cl-BSA, di-Cl-BSA, 4-Br-BSA, PSA, BSA, and *p*-TsOH.[86] The pKa values obtained for di-Cl-BSA, 4-Cl-BSA, 4-Br-BSA, PSA, BSA, and *p*-TsOH were found to be -3.33, -2.94, -2.85, -2.59, -2.36, and -2.14, respectively. These results show that halogen-substituted hydrotropic acids have higher inherent acidities than their hydroxyl- and methyl-substituted counterparts.

The acidity of aqueous hydrotropic acid solutions can also be determined by measuring the proton concentration (mol/L [H^+]), which directly reflects their acid strength.[86] The proton concentration provides a direct measure of the acidity or acid strength of the solution. By comparing the measured proton concentrations of various hydrotropic acids, including 4-Cl-BSA, PSA, BSA, and *p*-TsOH, the study evaluated their relative acidity under experimental conditions. The acidity of the aqueous solution containing 72% aryl sulfonic acid was assessed using the proton concentration. The obtained proton concentrations (mol/L [H^+]) at 60 °C for 4-Cl-BSA, PSA, BSA, and *p*-TsOH were 0.85, 0.62, 0.55, and 0.59, respectively, indicating that the 4-Cl-BSA solution was more acidic than the aqueous PSA, *p*-TsOH, and BSA solutions. The greater acidity and improved solubilization capabilities of the hydrotropic solvents resulted in better separation of lignin from poplar chips, i.e., 4-Cl-BSA and PSA demonstrated near-complete dissolution of lignin in poplar chips under the same set of conditions.[86] Conversely, 4-Br-BSA, di-Cl-BSA, BSA, and *p*-TsOH achieved lower percentages of lignin dissolution.[86] The observed differences in fractionation performance were attributed to the acidity of the aqueous hydrotropic acid solutions, where even slight variations in acidity had notable effects. For instance, the slightly higher acidity of the aqueous PSA solution (0.62 mol/L [H^+]) compared to the aqueous BSA and *p*-TsOH solutions (0.55–0.59 mol/L [H^+]) resulted in significantly improved lignin dissolution performance.[86]

3.2 As a solvent

The role of hydrotrope as a solvent can be explained by their solubilization, clustering, and aggregations of solute (**Fig. 8**). For instance, the structure of acid hydrotropes like PSA leads to a unique behavior in water due to the hydrophobic benzene ring and the hydrophilic phenolic

hydroxyl and sulfonic acid groups.[20] It can form clusters and aggregate in various forms, including (PSA)$_n$ aggregates, (PSA)$_n$ clusters, PSA-(water)$_n$ clusters, and PSA-(water)$_n$-PSA clusters. These formations are driven by the hydrophobic effect and occur at a critical aggregation concentration (C$_{ac}$). The aggregates of PSA orient their hydrophilic phenolic hydroxyl and sulfonic acid groups outward toward the water while the hydrophobic benzene ring is shielded inside (**Fig. 8a**). This arrangement allows the PSA aggregates to solubilize hydrophobic lignin fragments temporarily. The solubilization process involves reversible binding facilitated by the hydrophobic effect, π–π stacking, and π–polar interactions. The dilution of the PSA solution results in the breakup of the aggregates to facilitate the separation and recovery of the solubilized lignin as well as PSA. The solubilized lignin fraction that is protected by PSA has more inter-unit connections and higher molecular weight than the deposited lignin fraction. PSA demonstrated unique solubility and other solvent properties that enabled it to effectively dissolve and protect lignin fragments during the fractionation of biomass.

In the biomass fractionation process, lignin is considered a hydrophobic solute once it is depolymerized and isolated. He et al. used the sigma profile to confirm the hydrophobic nature of lignin model compounds as well as 4-Cl-BSA, and the results were used to explain the lignin solubilization in the applied hydrotrope.[86] The hydrophobicity of lignin was analyzed using log P and sigma profiles shown in **Figs. 5 and 8b**, respectively. Compared with the water molecule, the lignin dimer model compounds provided from 1 to 4 of log P, and their sigma profiles are located mostly in the non-polar region, unlike the water molecule, which showed a hydrogen bonding region.[86] Furthermore, the plot of the sigma profile for 4-Cl-BSA served amphiphilicity of hydrotrope in detail (**Fig. 8c**). Most of the peaks were calculated in non-polar region, but a peak of hydrogen bonding donor region was also presented.
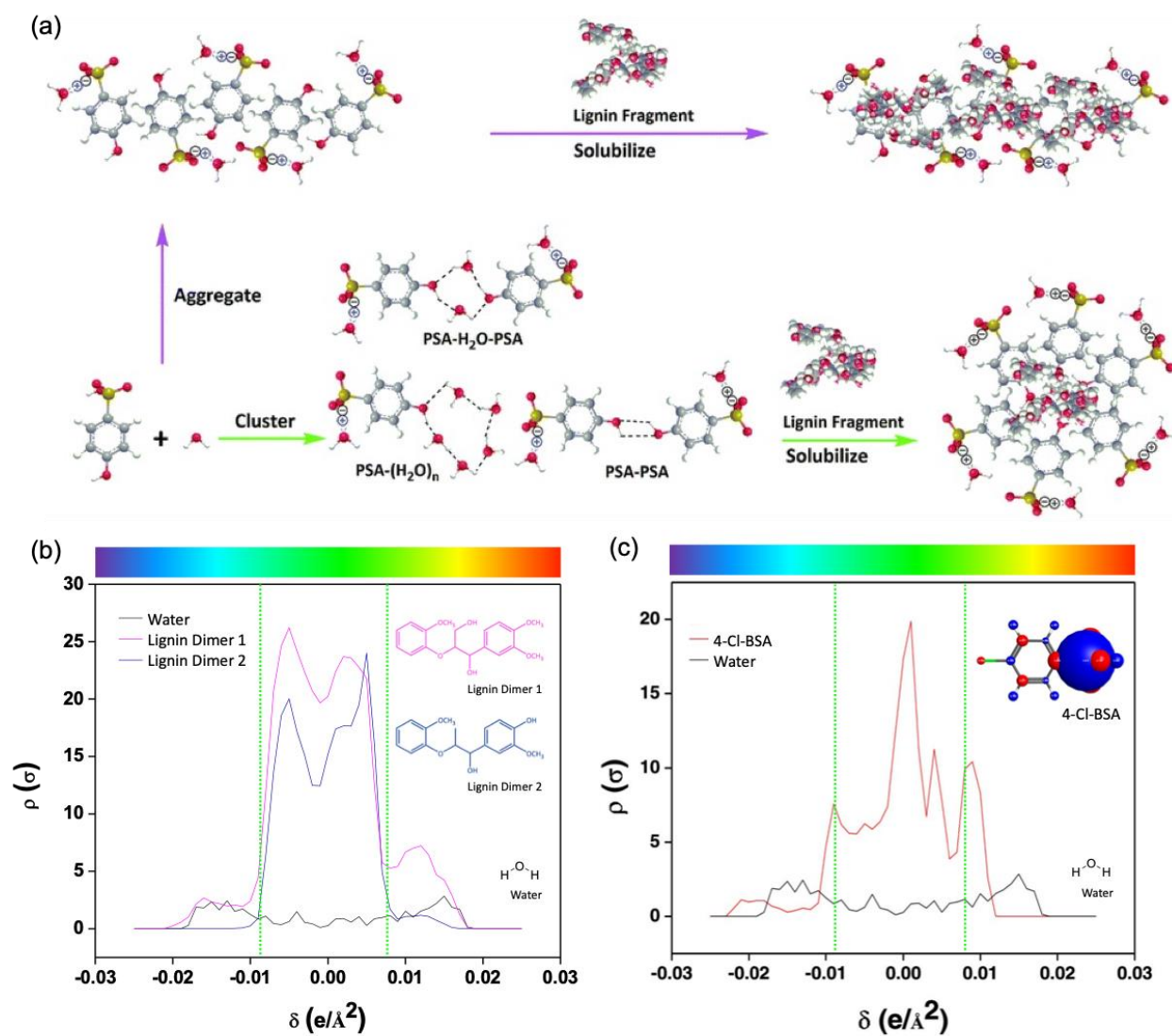
Fig 8. (a) A schematic illustration of the aggregation and clustering of PSA and the solubilization of lignin by PSA and sigma profiles of water, (b) lignin model compound, and (c) 4-Cl-BSA and its partial charge diagram.[20, 86] Adapted with permission from 89. Copyright 2021 American Chemical Society.

3.3 As a functionalizing agent

Besides as a catalyst and a solvent, hydrotropes can be a functionalizing agent in plant biomass utilization. Carboxylation can enhance the hydrophilicity and solubility of lignin due to the hydrophilic property of carboxyl groups. MA can act as an effective functionalization agent by introducing carboxyl groups onto the lignin structure, facilitating the formation of ester bonds between MA and lignin. Cai et al. developed an efficient biomass fractionation approach through lignin carboxylation using MA at atmospheric pressure and ≤100 °C.[49] The examination of the reaction products involving the lignin model compound, guaiacylglycerol-beta-guaiacyl ether, and MA via nuclear magnetic resonance (NMR) analysis confirmed the successful esterification of lignin with MA through the γ-OH group. MA hydrotropic fractionation (MAHF) introduces a surface charge alteration through the carboxylation of lignin, effectively reducing nonproductive cellulase binding due to electrostatic repulsion through pH mediation[112] and a low degree of condensation.[50] Lignin carboxylation also further enhances the lubrication effect of lignin during the production of lignin-containing cellulose nanofibrils through mechanical fibrillation. The MAHF method can generate highly dispersible, light-colored dissolved lignin with low condensation through carboxylation. Therefore, modified lignin with carboxyl groups exhibits versatility, potentially interacting with chemicals and substances.

4.   Application of hydrotropes for biomass processing

Acid hydrotropic processing has been introduced as an effective plant biomass fractionation technology by primarily dissolving lignin and hemicelluloses.[21] This section provides a comprehensive summary of the fractionation efficiency and characteristics of the recovered

lignin, hemicelluloses, and cellulose, as well as the conversion yields of carbohydrate fractions, along with their diverse applications.

4.1 *p*-Toluenesulfonic acid (*p*-TsOH)

Among several acid hydrotropes, *p*-TsOH was first introduced as a biomass processing solvent, which has strong hydrotropic properties toward lignin.[21] *p*-TsOH is a hydrophilic aromatic acid known for its stability and non-oxidizability.[113] The sulfonic acid group in *p*-TsOH acts as a hydrophilic tail, catalyzing the cleavage of ether and ester bonds.[21] The toluene group provides the hydrophobic property that interacts with the hydrophobic aromatic rings of lignin, facilitating the formation of aggregates through hydrophobic interactions.[5, 6, 21] It has been applied to the conversion of various biomass feedstock and generally resulted in effective delignification (**Table 1**).

4.1.1 Single-step *p*-TsOH processing for biomass pretreatment/fractionation

Chen et al. were the first to report the application of *p*-TsOH for biomass fractionation.[21] *p*-TsOH enabled the effective separation of components in poplar (NE222) under relatively mild conditions, including low temperature (80 °C) and short reaction times of around 20 min. This hydrotropic fractionation resulted in a delignification of more than 90% and xylan dissolution of more than 85% from poplar. Furthermore, the *p*-TsOH pretreatment exhibited solid substrate cellulose enzymatic digestibility (SED) of over 90% and also facilitated the generation of lignin nanoparticles. Cheng et al. produced acid hydrotrope-dissolved lignin that well preserved β-O-4 linkage (～60%), with a high molecular weight (～4000 Da) and a low glass transition temperature under moderate reaction conditions (i.e., ≤80 °C for ≤30 min), similar to milled wood lignin

(MWL).[114] Li et al. applied aqueous *p*-TsOH for delignification of different biomass including reed (*Phragmites communis*), hardwood (hybrid poplar), and softwood (*Radiata* pine).[115] Among three biomass, the highest delignification was made with reed by this hydrotropic solvent.

The hydrotropic fractionation process with *p*-TsOH solubilized xylan and further dehydrated into furans.[21, 52, 116] Zhu et al. also demonstrated a successful fractionation of poplar wood (*Populus deltoides Bartr. ex Marsh × Populus nigra* L.) into a water-insoluble cellulosic solid (WIS) and lignin- and xylose-rich spent liquor.[52] The highest ethanol concentration (52 g/L) was achieved from the WIS (**Fig. 9a**), and up to 78% furfural yield at a concentration of 6 g/L was obtained through direct dehydration of the spent liquor (containing *p*-TsOH) without additional catalyst. Yüksel et al. investigated the effectiveness of aromatic sulfonic acids as a catalyst for levulinic acid (LA) production from safflower stalk and reported that *p*-TsOH yielded the highest LA production at 88 g/kg biomass.[117]

For predicting xylan dissolution and delignification during *p*-TsOH processing, a reaction kinetic-based combined hydrolysis factor (CHF)[118] and combined delignification factor (CDF) were applied together.[114, 119] These kinetics-based reaction severity factors are useful for process scale-up and have been applied in several studies.[50, 120, 121] Yin et al. fractionated and characterized rice straw hydrotropic lignin using *p*-TsOH with varying combined delignification factor (CDF) (**Fig. 9b**).[122] The authors discussed the correlation between delignification reaction rate and CDF. The higher CDF signified the overall severity of the reaction, and the result showed that the lignin removal leveled at large CDF values. The hydrotropic lignin showed well-preserved β-O-4 linkage content (15–34%), high olefin content (21–69 olefin carbon in 100 total aromatic rings) that reflects lignin reactivity, and a low glass transition temperature (T_g) ranged 107–125 °C in a certain

CDF (severity) ranges. The phenolic OH of fractionated lignin significantly increased at large CDF values, suggesting the cleavage of β-O-4 linkage.

The quality of the recovered lignin is as important as yield. To understand the mechanism of lignin acidolysis, Feng et al. analyzed the structure of bagasse lignin before and after *p*-TsOH fractionation by NMR analysis.[123] This solvent achieved a remarkable 89% lignin removal. Cleavage of the β-O-4 structures of lignin during the acidolysis process resulted in the production of phenols and Hibbert ketones as byproducts, indicating that lignin underwent acidolysis during the *p*-TsOH pretreatment. The presence of sulfonated compounds in the soluble lignin like di-*o*-tolusulfone and di-*p*-tolusulfone suggest sulfonation reactions remains relatively insignificant during the *p*-TsOH pretreatment. After the *p*-TsOH pretreatment, β-β bonds were no longer detectable, and the β-5 bond existed in the lignin fraction at a low content of 3.28%. Wang et al. also reported similar lignin structural properties.[124] This suggests that the *p*-TsOH pretreatment can limit lignin condensation and enable the clean separation of lignin.

Ji et al. compared the delignification capacities of various solvent systems, including 70 wt% *p*-TsOH hydrotrope, DES (ChCl:lactic acid = 1:9, mass ratio), and [Amim][Cl].[125] *p*-TsOH hydrotrope resulted in the highest lignin removal, effectively solubilized 86% of lignin. The solubilized lignin exhibited a relatively high S/G ratio of 2.87. Thermogravimetric analysis (TGA) of the milled wood lignin (MWL, native form) and *p*-TsOH-extracted lignin (*p*-TsOHL) revealed that the TGA weight loss profiles of *p*-TsOHL closely resembled those of MWL. Well-preserved β-O-4 linkages during the fractionation were also confirmed with *p*-TsOHL by semi-quantitative NMR analysis.
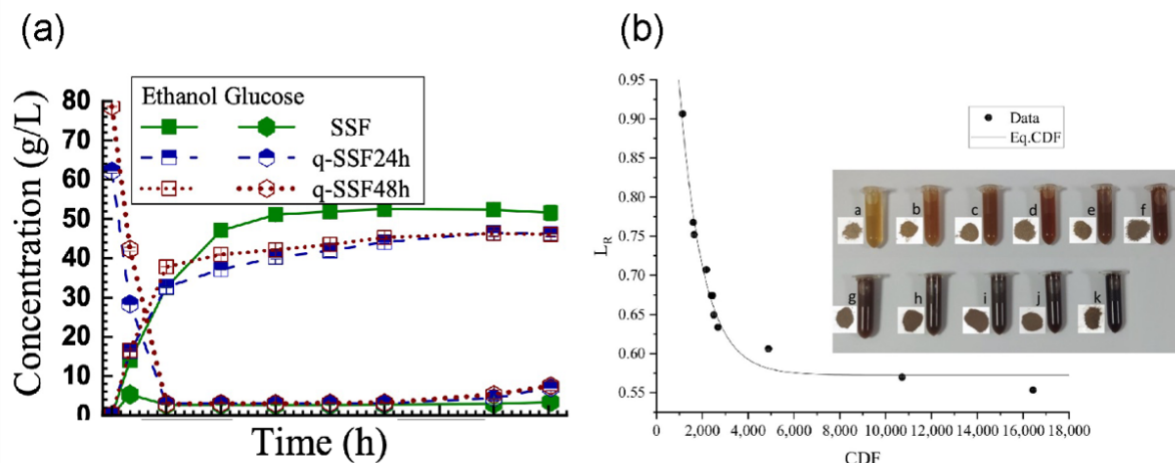
Fig. 9. Performance and application of fractionated components by *p*-TsOH. (a) ethanol production from poplar wood[52] and (b) combined delignification factors (CDF) of straw hydrotropic lignin.[122]

In addition, Ma et al. used 15 wt% of *p*-TsOH for the direct production of lignocellulosic nanofibrils (LCNFs) from wheat straw via effective delignification (**Fig. 10a**).[119] The resulting LCNFs were used to create films with exceptional mechanical properties, including a specific tensile strength exceeding 120 kN·m/kg. The study also showed that lignin nanoparticles (LNPs) were readily obtained from the spent liquor by water dilution (**Fig. 10b**). The acid hydrotrope, *p*-TsOH, also served as a catalyst and facilitated the conversion of the dissolved xylan into furfural with a yield of 57%. Yang et al. produced activated carbon (AC) using simple phosphoric acid activation with a high surface area of 2015 m^2/g using low sulfur acid hydrotropic lignin (AHL) from Poplar NE222.[126] The levels of surface area (2015 m^2/g) achieved were comparable to those of commercial alkali lignin (softwood, 2119 m^2/g) and lignosulfonate (2179 m^2/g). The study showed that the ACs produced using H$_3$PO$_4$ at a moderate temperature of 450 °C exhibited excellent adsorption performance, especially for Congo red and methylene blue dyes.

A desired biorefinery should valorize all biomass components. Zhu et al. applied *p*-TsOH hydrotropic fractionation and co-produced bioethanol, furfural, and LNPs from birch wood.[127] They achieved a bioethanol yield of 76% from the glucan-rich washed WIS fraction and a furfural yield of 78% from the xylose-rich spent liquor by dehydration without additional catalyst. In addition, LNPs with an average particle size of 37 nm were obtained from the enzymatic hydrolysis solid residue.

Table 1. Biomass fractionation performance and product properties by *p*-TsOH.

Biomass	Pretreatment condition	Fractionation Performance	Product Properties	Ref.
Poplar (NE222)	• 80 °C; 20 min	• Delignification : 90%	• Substrate cellulose enzymatic digestibility (SED) of glucan: 90%	21
	• 90 °C; 112 min	• Hemicellulose removal : 79% • Delignification : 84%	• Ethanol conc. : 52.47 g/L • Furfural conc. : 6.18 g/L • Furfural yield : 78%	52
	• 80 °C; 20 min	-	• Surface area of lignin-based activated carbon : >2000 m^2/g	126
	• ≤80 °C; ≤30 min	-	• Content of β-O-4 linkage content: ~60% • M_w: ~4000 Da	114
Radiata pine	• 80 °C; 30 min	• Cellulose loss : 18% • Hemicellulose removal : 65% • Delignification : 28%	• Content of β-O-4 linkage: 54% • Content of β-5 linkage : 43% • Note: based on total β-O-4, β-5 and β-β as 100%	115
Hybrid poplar	• 80 °C; 30 min	• Cellulose loss : 13% • Hemicellulose removal : 80%	• Content of β-O-4 linkage: 60% • Content of β-5 linkage : 34%	

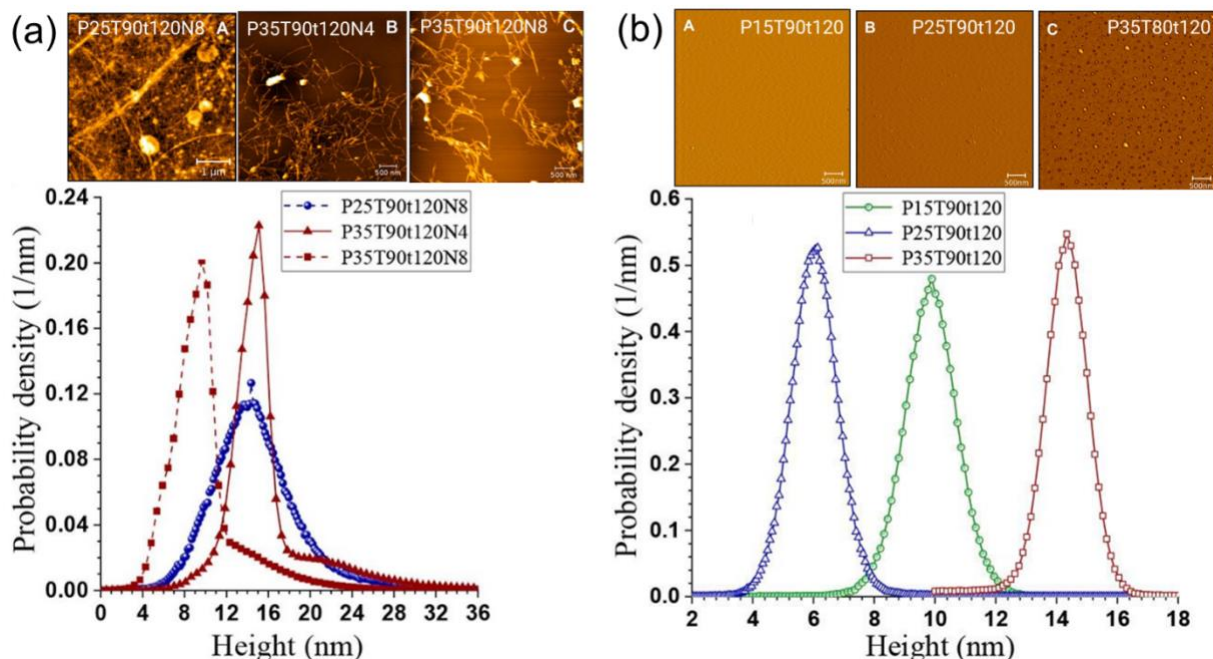|		• Delignification: 51%	• Note: based on β-O-4, β-5 and β-β as 100%	
Reed	• 80 °C; 30 min	• Cellulose loss : 9% • Hemicellulose removal : 86% • Delignification : 78%	• Content of β-O-4 linkage: 60% • Content of β-5 linkage : 34% • Note: based on β-O-4, β-5 and β-β as 100%	
Safflower stalk	• 200 °C; 120 min	-	• Maximum LA yield: 88 g LA/kg biomass	[117]
Rice straw	• 60–80 °C; 15–60 min	• Delignification : 18–52%	• Content of β-O-4 linkage: 15–34% • Note: based on 100 aromatic units • Low T_g (107–125 °C)	[122]
Bagasse	• 80 °C; 20 min	• Delignification : 89%	• β-5: 3.28% • Note: based on 100 aromatic units	[123]
Hybrid poplar	• 80 °C; 90 min	• Cellulose loss : 14% • Hemicellulose removal : 77% • Delignification : 86%	• S/G ratio: 2.87 • β-O-4: 79% • β-5: 14% • β-β: 8% • Note: based on β-O-4, β-5 and β-β as 100%	[125]
Wheat straw	• 90 °C; 120 min	• Composition - Cellulose: 55% - Hemicellulose : 9% - Lignin: 17%	• LCNF Film: specific tensile strength over 120 kN·m/kg • LNPs: easily precipitated with water • Furfural yield: 57%	[119]
Birch wood	• 90 °C; 180 min	• Composition - Cellulose: 61% - Hemicellulose : 10% - Lignin: 22%	• Ethanol yield: 76% • Furfural yield: 78% • Average particle size of LNPs: 37nm	[127]

"-": not reported

Fig. 10. Performance and application of *p*-TsOH using biomass processing. (a) atomic force microscopic (AFM) images of lignocellulosic nanofibrils (LCNFs) and AFM measured their height distributions, (b) AFM images of lignin nanoparticle (LNPs) and dynamic light scattering measured particle size distributions.[119] Adapted with permission from 124. Copyright 2018 American Chemical Society.

4.1.2 Synergistic effect of *p*-TsOH processing for biomass utilization

Although *p*-TsOH showed effectiveness for biomass fractionation, its efficiency can be further improved by integrating physical and/or chemical treatment methods.[128] **Table 2** shows the performance of subsequent conversions of the fractionated biomass component from *p*-TsOH in conjunction with other processing approaches. Zeng et al. developed a freeze-thaw-assisted pretreatment method with *p*-TsOH for effective separation of bagasse lignin.[128] The method showed high extraction efficiency (78%) and purity (78%) of the separated lignin. Freeze-thaw

leads to effective lignin separation while preventing oxidative degradation of lignin and hemicellulose dissolution. Consequently, the process yields high-purity lignin with elevated molecular weight. The research conducted by Peng et al. also investigated the effectiveness of freeze-thaw-assisted p-TsOH (F/p-TsOH) pretreatment in hemicellulose separation from bamboo.[129] In comparison with traditional p-TsOH pretreatment, F/p-TsOH pretreatment enhanced hemicellulose separation yield by 33%. The freeze-thaw pretreatment allowed the decrease of acid concentration and reaction temperature in the hemicellulose separation process; therefore, the dissolution of cellulose and lignin was reduced.

Ma et al. applied ball-milling before p-TsOH for the pretreatment of reed.[130] The inclusion of ball-milling in the pretreatment process improved enzymatic hydrolysis efficiency. Compared with the condition without ball milling (glucan digestibility: 75%), when samples were pretreated with a combination of p-TsOH (at concentration 55 wt%) and ball milling (55BM), the glucan digestibility of the pretreated residue was 86%. The enzymatic hydrolysis residue was used for the composite application. The residue was mixed with polylactic acid (PLA) and extruded a residue-plastic composite (RPC). The RPC demonstrated a bending strength of 29 MPa, Young's modulus of 583 MPa, bending modulus of 879 MPa, and impact strength of 13 kJ/m^2. BRPC (ball-milling residue-plastic composite) showed better impact strength (17 kJ/m^2) than RPC, since ball-milling residue had a larger surface area, enabling better interaction between biomass and PLA, ultimately enhancing impact strength.

Zhu et al. combined hydrothermal pretreatment (HP) with subsequent acid hydrotropic pretreatment (AHP) to selectively fractionate xylooligosaccharides (XOS), fermentable sugars and LNPs from poplar.[51] In the first step, 6.7 g/L of XOS in the range of X2 (xylobiose)–X6 (xylohexaose) was extracted from raw xylan through HP at 170 °C for 50 min. Subsequently, LNPs

averaging 44.8 nm in size were generated from the HP pretreated poplar, using p-TsOH at a concentration of 55% (w/v) at 90 °C for 120 min. A high rate of glucan preservation (96%) was achieved by HP-AHP pretreatment. To remove residual surface lignin particles present on the surface of HP-AHP pretreated poplar, 0.1% NaOH was applied, resulting in a significantly improved enzymatic hydrolysis yield (97%). This approach improved the overall utilization of poplar with XOS, fermentable sugars and LNPs as products.

Gu et al. performed a physicochemical treatment approach, employing autohydrolysis (H), disk refining (R), and p-TsOH hydrolysis (P) sequentially for the fractionation of poplar wood.[131] The combination of disk refining and p-TsOH pretreatment effectively increased the removal of lignin (>90%). The pretreated poplar of HRP and RP displayed a higher crystallinity index (CrI) of 78% compared to the raw material (61%), pretreated poplar of P (70%) and HP (74%). Lin et al. also developed a graded fractionation technique to efficiently extract XOS, nanolignin and nanocellulose from corncob.[132] This approach focuses on sequentially isolating the hemicelluloses, lignin and cellulose. First, formic acid-NaOH pretreatment was performed to produce a high yield of XOS (38%) from hemicellulose of corncob. The rapid dissolution of lignin can be facilitated by p-TsOH. As a result, nanoscale lignin particles with diameters less than 10 nm were successfully extracted using the p-TsOH. The solid residue was further processed using TEMPO oxidation to produce high crystallinity nanocellulose after p-TsOH fractionation. The resulting TEMPO-oxidized cellulose exhibits a 63% nanofibrillation ratio, with fibrils under 1 μm in length and width below 20 nm.

Table 2. Biomass fractionation performance and product properties by combination of *p*-TsOH and other processing methods.

Pretreatments & solvents	Biomass	Pretreatment condition	Fractionation Performance	Product Properties	Ref.

Freeze-thaw and *p*-TsOH pretreatment	Bagasse	• Freeze–thaw pretreatment
		  - Freezing temperature : -60 °C
		  - Freezing time: 8 h
		  - Thawing temperature : 15 °C
		• *p*-TsOH pretreatment : 70 °C; 20 min
			• Cellulose loss : 8%
			• Hemicellulose removal : 24%
			• Delignification :90%
				• High extraction (78%) and purity (78%)	128

	Moso bamboo	• Freeze–thaw pretreatment
		  - Freezing temperature : -40 °C
		  - Freezing time : 20 h
		  - Thawing temperature : atmospheric temperature
		• *p*-TsOH pretreatment :130 °C; 80 min
			• Cellulose loss : 11%
			• Hemicellulose removal : 93%
			• Delignification :14%
					129

Ball-milling and *p*-TsOH pretreatment	Reed	• Ball-milling : 300 rpm; 30 min • *p*-TsOH pretreatment : 90 °C; 30 min	• Cellulose loss : 23% • Hemicellulose removal : 95% • Delignification : 94%	• Enzymatic hydrolysis yield of glucan: 86%	130
Hydrothermal pretreatment, *p*-TsOH pretreatment	Poplar	• Hydrothermal pretreatment : 170 °C; 50 min • *p*-TsOH pretreatment	• Cellulose loss : 8% • Hemicellulose removal : 84%	• Concentration of xylooligosaccharides (X2–X6): 6.7 g/L • Average size of LNPs : 44.8 nm	51

and alkaline incubation		• : 90 °C; 120 min • Alkaline incubation 50 °C : 60 min	• Delignification : 77%		
Autohydrolysis, wood size reduction and p-TsOH pretreatment	Poplar NE222	• Autohydrolysis : 170 °C; 50 min • p-TsOH pretreatment : 80 °C; 20 min	• Delignification : 90%	• CrI: 78%	[131]
Formic acid–NaOH pretreatment, p-TsOH pretreatment and TEMPO	Corncob	• Formic acid treatment : 160 °C; 60 min • NaOH pretreatment : 160 °C; 60 min • p-TsOH treatment : 80 °C; 20 min • TEMPO : 60 °C; 72 h	-	• Xylooligosaccharides yield: 38% • Nanoscale lignin particles with diameters less than 10 nm • Nanofibrillation ratio of TEMPO-oxidized cellulose: 63%, less than 20 nm in width and less than 1 μm in length	[132]

"-": not reported

4.2 Other aromatic hydrotropic solvent

Besides p-TsOH, several hydrotropic solvents, such as bifunctional phenol-4-sulfonic acid, 5-sulfosalicylic acid (5-SSA), and benzenesulfonic acid (BA), were also applied in biomass processing. **Table 3** shows the fractionation performance and product properties using these hydrotropic solvents.

4.2.1 Phenol-4-sulfonic acid (PSA)

He et al. demonstrated that PSA can be used as a selective catalyst and mesoscale hydrotropic solvent.[20] This process showed a near complete fractionation of woody biomass without energy-intensive size reduction of biomass. PSA effectively fractionated hardwood chips

(1.0–2.5 cm in length, 0.8–1.5 cm in width, 0.3–0.6 cm in thickness) into high-quality cellulose fibers (length: >1 mm, crystallinity index: 61–65, degree of polymerization (DP_v): 830–887), hemicellulosic sugars, and lignin (delignification: 99%) under mild conditions (50–80 °C, 0.5–3.0 h, atm). The authors also claimed a potential "closed-loop" fractionation process by synthesizing lignin fragments to PSA via sulfonation. The PSA formed a cluster in water due to the hydrophobic effect, and the phenolic hydroxyl group and sulfonic acid group were adjusted with the water phase above critical aggregation concentration. The hydrophobic part of the hydrotrope was allocated with lignin fragments and dissolved in a hydrotropic solvent.[20, 21, 94, 133]

4.2.2 5-Sulfosalicylic acid (5-SSA)

Zhai et al. examined 5-SSA for fractionating poplar under mild aqueous conditions.[4] Optimum conditions, by 80 wt% aqueous 5-SSA solution at 110 °C for 60 min reaction, resulted in 70% lignin removal, 80% cellulose recovery, and 76% glucan digestibility. The density functional theory (DFT) calculation provided the non-covalent interaction between the 5-SSA and lignin model compound (LM). The authors reported that the strong hydrogen bonding interactions between the sulfonic acid group of 5-SSA and LM facilitated the disruption of hydrogen bonding networks in lignin fragments, ultimately leading to their breakdown, but also the dissolution of disintegrated LM in hydrotropic solvent due to their strong hydrogen bond interaction.

4.2.3 Benzenesulfonic acid (BA)

Dong et al. demonstrated the effective biomass fractionation by benzenesulfonic acid (BA) with approximately 80% delignification and 70% xylan removal under mild reaction conditions (80 °C and 20 min).[53] The authors produced lignocellulosic nanomaterials and sugars from the

cellulosic-rich solid fraction with 80% glucan digestibility. The study also found that the resulting LCNF had a number-averaged fibril height of 11 nm, measured from the residual lignin content. Furthermore, the collected spent acid liquor could be easily diluted with an anti-solvent to obtain lignin particles with a size of 203 ± 4 nm.

Yang et al. performed fractionation of eucalyptus wood using p-TsOH and BA.[54] The authors reported that the minimum hydrotrope concentration (MHC) of hydrotrope affects the separation of dissolved lignin from the solution. In this study, the MHC of p-TsOH and BA were 12% and 25%, respectively. Both hydrotropic solvents provided lignin purities of over 99%. BA processing resulted in a better lignin and xylan removal rate than p-TsOH treatment at the same hydrotrope concentration, while the molecular weight (4830–5440 g/mol of p-TsOH and 4390–4840 g/mol of BA) and homogeneities (Đ ≤2.15 of p-TsOH and Đ ≤1.91 of BA) of lignin were similar. The extracted lignin by BA had superior antioxidant activity than the commercial oxidant butylhydroxytoluene (BHT) and p-TsOH with a radical scavenging index (RSI) value of 0.29.

4.2.4 4-Chloro-Benzenesulfonic acid (4-Cl-BSA)

The presence of the electron-withdrawing chloro group in 4-Cl-BSA made it a stronger acid compared with PSA.[86] This strong acidity enables an easy fractionation of lignocellulosic materials at mild temperatures. Additionally, due to the hydrophobic properties of the chloro group, 4-Cl-BSA readily forms aggregates in water compared with PSA. These aggregates are less likely to cause substantial structural changes to the lignin particles deposited on cellulose fibers. He et al. developed a mild-condition fractionation process using 4-Cl-BSA to effectively fractionate unmilled poplar chips of approximately 1.0–2.5 cm (length) × 0.8–1.5 cm (width) × 0.3–1.0 cm (height) at 50–80 °C for 18–180 min.[86] The deposited lignin retained a substantial portion of native

lignin β-O-4 linkages (62–81%) and uncondensed aromatic units (78–86%). In comparison to various aryl sulfonic acids with or without substituents (such as dichloro, bromo, hydroxyl, and methyl) and mineral acids, 4-Cl-BSA proved superior under mild conditions, providing different aggregation and clustering behavior along with their own amphiphilicity which was measured by log P and sigma profile described in this study. The amphiphilicity and acidity of sulfonic acid in 4-Cl-BSA provided remarkable effectiveness in the fractionation and conversion of biomass.

Table 3. Biomass fractionation performance and product properties by other hydrotropic solvents.

Solvents	Biomass	Pretreatment condition	Fractionation Performance	Product Properties	Ref.
Phenol-4-sulfonic acid (PSA)	Poplar chip	• 50–80 °C; 30–180 min	• Delignification : 99%	• Directly applied to hardwood chips (1.0–2.5 cm in length, 0.8–1.5 cm in width and 0.3–0.6 cm in thickness) • Cellulose fibers of high quality (length : >1 mm, CrI : 61–65%, DP_v: 830–887)	20
4-Chloro-Benzenesulfonic acid (4-Cl-BSA)		• 50–80 °C; 18–180 min	• Delignification : >96%	• Directly applied to wood chips (1.0–2.5 cm in length, 0.8–1.5 cm in width and 0.3–1.0 cm in height) • β-O-4 linkages : 62–81% of native lignin • Uncondensed aromatic units : 78–86%	86
5-sulfosalicylic acid (5-SSA)	Poplar stem	• 110 °C; 60 min	• Cellulose loss : 20% • Hemicellulose removal : 85% • Delignification : 70%	• Enzymatic hydrolysis yield of glucan : 76%	4
Benzenesulfonic acid (BA)	Alkaline peroxide mechanical pulp (APMP) fiber	• 80 °C; 20 min	• Hemicellulose removal : ~70% • Delignification : ~80%	• Enzymatic hydrolysis yield of glucan : 80% • Number-averaged fibril height of LCNF : 11 nm • Lignin particles size : 203 ± 4 nm	53
	Eucalyptus wood	• 80 °C; 20 min	• Hemicellulose removal : 75-85% • Delignification : 50-83%	• Lignin purity : >99% • M_w: 4390–4840 g/mol • Đ ≤1.91	54

4.2.5 Salt-based aromatic hydrotropes

Some salt-based hydrotropes are still applied for biomass processing despite their ineffectiveness, as discussed earlier.[37] Sodium xylene sulfonate (SXS) was used for biomass pretreatment in recent studies.[46, 88, 134] Gabov et al. claimed SXS as an environmentally friendly hydrotropic agent in a single-stage fractionation of sugarcane bagasse that can produce high-quality cellulose pulp, lignin, and furfural (**Table 4**).[46] The process resulted in a pulp fraction with a yield of 45–67% with 60–92% cellulose content. The study also reported a lignin recovery yield of 12–15% with a purity ranging from 88–94% and a furfural yield of 1–8% (based on biomass weight) from the partial hydrolysis of hemicellulose. Qi et al. modified the SXS pretreatment method with pH adjusted to 3.5 by formic acid to improve enzymatic digestibility and achieved 12.41 g/L of Acetone-butanol-ethanol (ABE) from wheat straw.[88] Dawid et al. applied sodium cumene sulfonate (NaCS) with maize stillage biomass for ethanol production. The authors used microwave radiation to overcome the limitation of aqueous salt solution.[135] High concentrations of ethanol ($\geq$40 g/L) were obtained from biomass using this process, achieving 95% of the theoretical fermentation yield. This microwave-assisted hydrotropic fractionation method removed 44% of lignin from biomass without generating any fermentation inhibitors. Nonetheless, these salt-based hydrotropes demonstrated a relatively low efficiency in lignin removal compared to the aforementioned acid hydrotropes[135] because the solubility of dissociate compounds in water is affected by the salting in and salting out effect.[28, 34]

Table 4. Biomass fractionation performance and product properties by salt-based aromatic hydrotropes.

Pretreatments & solvents	Biomass	Pretreatment condition	Fractionation Performance	Product Properties	Ref.
Sodium xylene sulfonate (SXS)	Sugarcane bagasse	• 150 and 170 °C; 60 and 120 min	• Delignification : 50–93%	• Pulp yield : 45–67% • Lignin recovery yield : 12–15% • Furfural yield : 1–8%	46
	Wheat straw	• 160 °C; 60 min	-	• Acetone-butanol-ethanol (ABE) : 12.41 g/L	88
Microwave-assisted pretreatment with NaCS	Maize stillage biomass	• 117 psi (pressure); 30 min	• Delignification : ~44%	• Fermentation yield : 95% • Ethanol concentration : ≥40 g/L)	135

"-": not reported

4.3 Aliphatic acid hydrotropic solvent (maleic acid)

MA, a dicarboxylic acid, can be categorized as an aliphatic hydrotrope. It is approved as an indirect food additive by the U.S. Food and Drug Administration (FDA, 21CFR175-177), making it safe for food-related applications and its potential in biomass biorefinery processes.[40, 49] It has a lower acidity (pKa=1.9, much less corrosive) than p-TsOH and other sulfonic acids, which can significantly decrease environmental impact and capital costs in biomass biorefinery operations.[6, 40] MA has a relatively lower solubilization capacity than p-TsOH due to its lower acidity. MA has a higher MHC of (25 wt%) compared with p-TsOH of 11.5 wt%, making it advantageous for acid recovery.[6, 40] The relatively high MHC of MA requires less water consumption for lignin precipitation and less energy requirements for water distillation for its

recovery. Moreover, it can produce sulfur-free lignin, addressing the issues of sulfur, metal, and ammonia cations often found in commercial technical lignins obtained from sulfite and sulfate pulping processes.[126] This helps mitigate negative environmental effects associated with the release of sulfur and ammonia during activation. Additionally, carboxylation of lignin by MA can enhance the surface charge of lignin and minimize nonproductive cellulase binding to lignin by creating electrostatic repulsive interaction between cellulase and lignin. Dissolution of lignin by MA increases its hydrophilicity and exhibits high dispersion.

Su et al. also applied MAHF to fractionate switchgrass at atmospheric pressure and reported the improved enzymatic digestibility of the fractionated cellulosic WIS.[50] The glucan digestibility of MAHF WIS was up to 79%, which was higher than the *p*-TsOH fractionated one (54%). MAHF also made higher antioxidant activity of the dissolved lignin and more effectively facilitated the mechanical fibrillation of WIS into nanofibrils than that from *p*-TsOH (**Fig. 11**). They also discussed that MAHF would be a more sustainable option for fractionation than *p*-TsOH because MA is an FDA-approved indirect food additive. Additionally, the lower acidity and solubility of MA can reduce water usage for lignin precipitation and minimize water distillation needed for acid recovery. The study further confirmed the findings in a comparative study between *p*-TsOH and MA for fractionation of birch wood.[40]
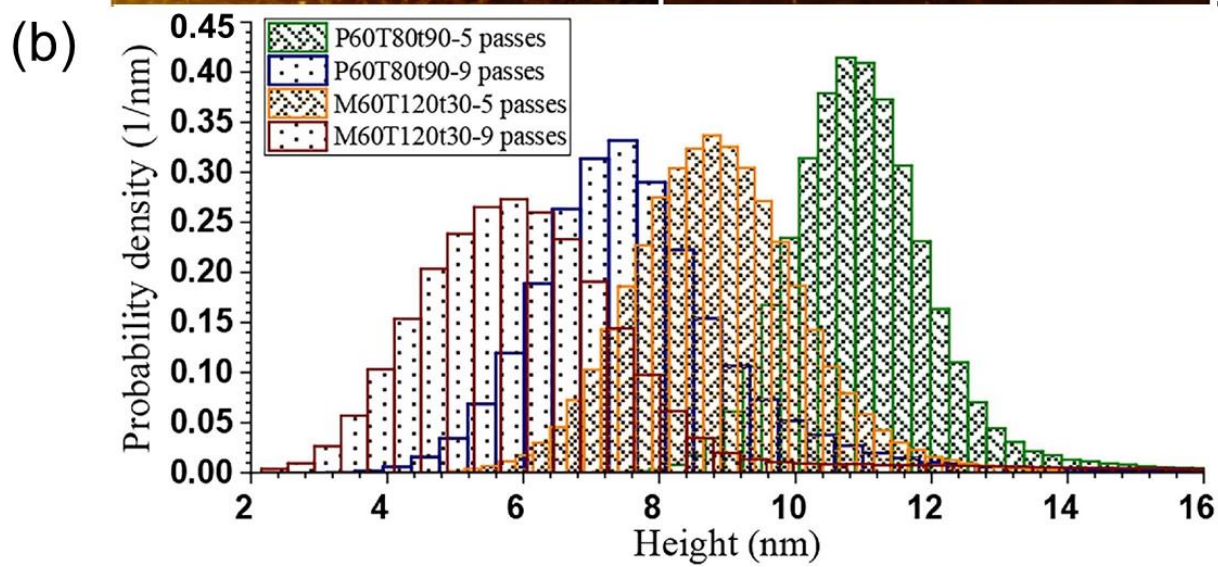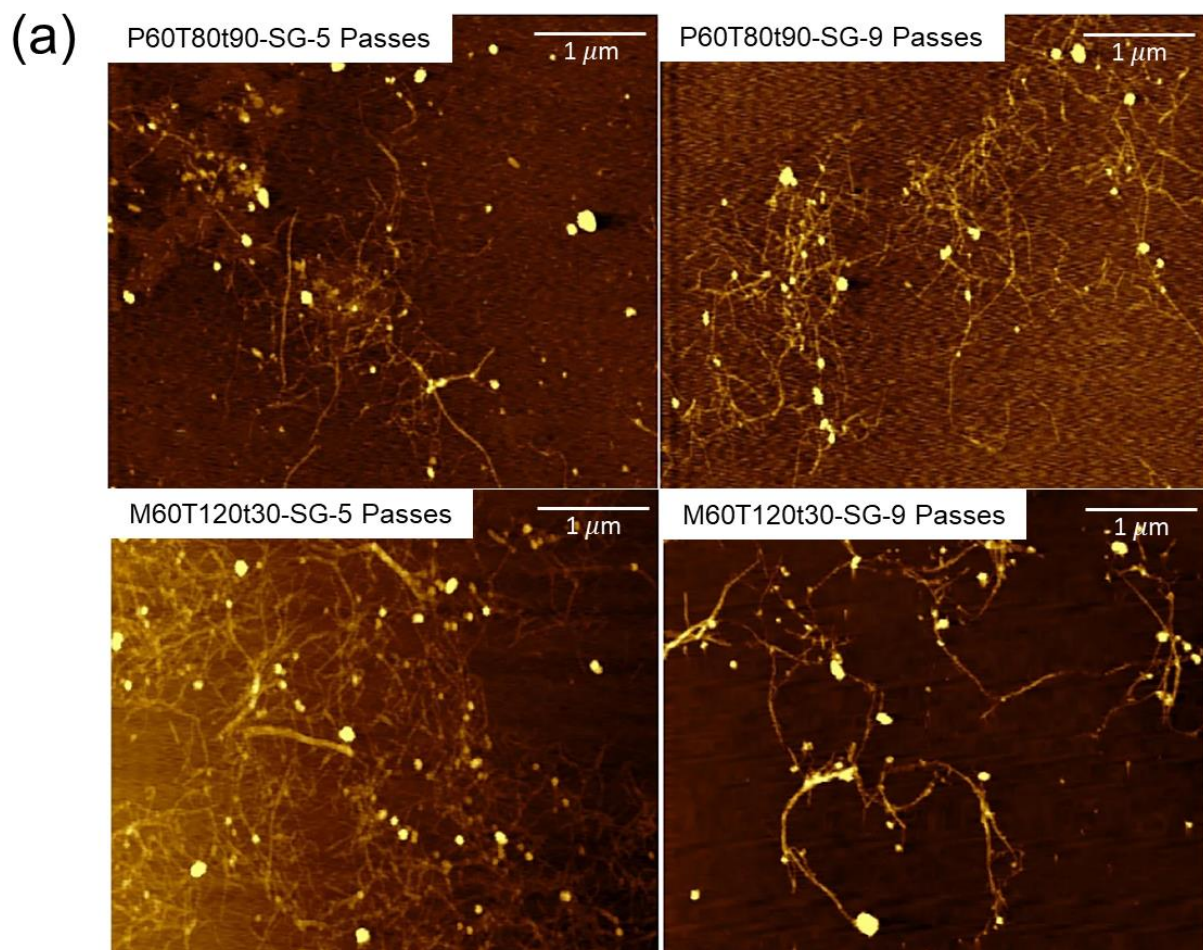
(a)

P60T80t90-SG-5 Passes   1 μm   P60T80t90-SG-9 Passes   1 μm

M60T120t30-SG-5 Passes   1 μm   M60T120t30-SG-9 Passes   1 μm

(b)

P60T80t90-5 passes
P60T80t90-9 passes
M60T120t30-5 passes
M60T120t30-9 passes

Fig. 11. AFM images of LCNFs from AHF WISs (a) using *p*-TsOH and MA and varied passes through microfluidization along with their AFM topography-measured (b) LCNF height probability distributions.[50]

4.4. Ionic liquids

Some ionic liquids (ILs) functioned as important hydrotropes and resulted in the improvement of the solubility of hydrophobic compounds, such as phenolic acids in biomass. Cláudio et al. investigated a series of ionic liquids as a catanionic hydrotrope and reported their effects on selective solubilization of biomass components.[28] The solubility of extracted gallic acid and vanillin from biomass in pure water and pure ionic liquids showed a 40-fold increase in solubility in the presence of pure ionic liquids compared to pure water. The authors discussed that the formation of solute-IL aggregates enhanced the sparingly soluble organic compounds. The formation of aggregates between vanillin and the ionic liquid within the solution was confirmed by DLS analysis. De Faria et al. investigated the potential of aqueous solutions of ILs solutions as alternative solvents for the extraction of triterpenic acids (TTAs) from apple peels.[27] The solubility of ursolic acid (UA), as a major representative of TTAs, increased by 8 orders of magnitude in aqueous IL solutions compared to pure water. The TTAs extraction yields obtained from apple peels resulted in higher total extraction yields of 2.62 wt% compared to extraction yields ranging from 1.37 wt% to 2.48 wt% when chloroform and acetone were used under similar conditions.

4.5. The impacts of hydrotropic solvent structure on their performances

Hydrotrope can vary in the bulk structure (e.g., benzene, tetrahydrofuran, γ-valerolactone, aliphatic), the number, position, hydrophobicity/hydrophilicity, and electron affinity

(withdrawing/donating) of non-acid substituent (e.g., halogen, alkyl, hydroxyl, amine), and the number and type (carboxylic acid, sulfonic acid) of the acid substituent (**Figs. 2 and 5**). As discussed throughout this manuscript, these structural variables of hydrotrope affect its properties (amphiphilicity, clustering/aggregation behavior, water-solubility, acidity, and recyclability) and performance (as hydrotropic solvent, catalyst, and functionalizing agent) during biomass processing. Hydrotropes with hydrophobic substituents such as halogen and alkyl tend to aggregate/cluster in water at lower concentrations but have lower water solubility.[86] Hydrotropes with hydrophilic substituents such as hydroxyl, amine, carboxylic acid, and sulfonic acid can have better water solubility (**Fig. 5**). Hydrotropes with electron-withdrawing halogen substituents (choro- and bromo-) are inherently more acidic than hydrotropes with electron-donating substituents (hydroxyl and alkyl) (**Fig. 5**). Hydrotrope with strong acidity and a good water solubility usually acts as an efficient catalyst in biomass processing. Hydrotropes with carboxylic acid can functionalize lignin by reacting with it during biomass processing (**Fig. 7**).[49] However, these speculations need to be further validated through comprehensively investigating structural properties and performances of a wide range of hydrotropes with systematically varied structures. The structure of the applied hydrotrope affects its properties including acidity as well as biomass pretreatment performance such as the degradation and/or separation of cellulose and lignin. The fractionation behavior determines the fractionated biomass substrate morphological changes such as the substrate specific surface area and the pore size, affecting substrate enzymatic digestibility.[53, 136] Also, the inherent capacity of hydrotropes to effectively reduce liquid surface tension serves as an effective reaction solvent due to its amphiphilicity. In particular, the aggregation behavior of hydrotrope is beneficial to precipitate lignin with water dilution after delignification.[75]

Cai et al. compared the effectiveness of MA and *p*-TsOH for the acid hydrolysis of birch wood.[40] As shown in **Fig. 5**, *p*-TsOH has a higher log P value (1.68) than MA (-0.36) due to its aromatic ring and methyl group. These structural properties of MA and *p*-TsOH had distinct impacts on several aspects of biomass pretreatment. Due to its higher hydrophobicity, *p*-TsOH showed a better lignin dissolution than MA. However, the fractionated lignin by MA had more β-O-4 linkages with less condensed structure because of its weaker acidity (pK_a of MA = 1.9; pK_a of *p*-TsOH = -2.8) as well as protection of β-O-4 linkages by MA esterification. The MA fractionated lignin resulted in higher monophenol yields and more uniform molecular weight distribution. The dissolved lignin by MAHF also had a lighter color than the lignin fractionated by *p*-TsOH, which had more condensed structures and chromophore groups. The residual lignin in MA-fractionated WIS was also carboxylated and had less nonproductive cellulase binding; therefore, its enzymatic hydrolysis was improved. For instance, the enzymatic digestibility of WIS-MT$_{120}$ (MA at 60 wt % and 120 °C for 30 min) was 95% at a low cellulase loading of only 10 FPU/g glucan, while WIS-PT$_{85}$ (*p*-TsOH at 60 wt % and 85 °C for 20 min) had 48% digestibility, despite these two substrates had almost identical chemical composition. Moreover, nanofibrillation of the WIS was facilitated by MA carboxylation of lignin and resulted in LCNFs with a diameter/height of 16 nm and lower fibrillation energy, while *p*-TsOH produced a larger size of LCNFs with a greater than mean diameter/height of 23 nm.

5. Synergistic effect of hydrotrope in co-solvent system

Acid hydrotrope fractionations generally have milder reaction conditions in terms of reaction temperature and reaction duration than other biomass processing approaches, but they still result in the undesired modification of biomass components. Due to the heterogeneity of biomass,

a single bioprocessing method cannot be optimized for the entire biomass components; therefore, compromised reaction conditions were determined based on the priority of the target products. A combination of different technologies can have synergistic effects on biomass processing by reducing chemical and energy consumption and/or improving the efficiency of biomass conversion. The fractionation performance and properties of biomass using hydrotropic pretreatment in conjunction with other processing approaches are presented in **Table 5**.

Fan et al. developed a green acid-catalyzed fractionation process using 0.5 to 3.0 mol/L *p*-TsOH/ethanol for lignin extraction from lignocellulosic biomass while preserving carbohydrate components.[137] Compared to other acids such as hydrochloric acid, sulfuric acid, and formic acid, *p*-TsOH showed superior lignin extraction efficiency under the same condition. The process yielded 84% of lignin from poplar sawdust, preserving high cellulose (99%) and hemicellulose (50%) contents by 3.0 mol/L *p*-TsOH at 85 °C. The extracted lignin exhibited a noncondensed structure and showed molecular weight in the range of 2070 to 2630 g/mol, a narrow molecular weight distribution (Đ: 1.94–2.46), and an S/G ratio range of 1.82 to 2.71. The interaction of *p*-TsOH with lignin through aromatic-aromatic and hydrophobic interactions facilitated lignin release without carbohydrate degradation. Moreover, the addition of ethanol minimized the re-condensation of the extracted lignin. These findings highlight the potential of this acid-catalyzed process for the selective extraction of lignin with desirable properties from lignocellulosic biomass. In addition, the authors showed >94% recoveries of *p*-TsOH with three-cycle processing to demonstrate its potential economic feasibility. Similarly, Zhai et al. developed a methanolysis pretreatment strategy using *p*-TsOH as a recyclable catalyst for fractionating bamboo fiber.[138] The authors claimed the high solubilities of *p*-TsOH and biomass components in methanol and its quenching effect to reduce lignin repolymerization as the advantages of their process. The

optimized conditions (110 °C, 30 min, and 10% p-TsOH) resulted in efficient dissolution of lignin (88%) and xylan (90%) while retaining a high cellulose content (87%) in the pretreated bamboo. Enzymatic hydrolysis of the pretreated bamboo achieved a yield of 89% with a cellulase loading of 15 FPU/g glucan, significantly higher than that of untreated bamboo. The extracted lignin exhibited the preferred properties with low dispersity (1.80), high purity (>94%), and moderate molecular weight (3472 g/mol of M_w), while hemicelluloses were mainly converted into methyl xyloside (10%). This strategy shows potential for large-scale fractionation of cellulose pulp, lignin, and methyl xyloside from lignocellulosic biomass.

Madadi et al. introduced the mannitol (MT)-assisted p-TsOH/pentanol (p-TsOH/pentanol/water, 20:60:20 wt%) pretreatment to improve the fractionation of poplar chip.[139] By adding 5% MT in the pretreatment solvent, delignification and surface area of biomass were significantly increased, leading to a glucose yield of 95% at a low cellulase loading of 7.5 FPU/g glucan and a high furfural yield of 84%. The fractionated lignin had well-preserved intact lignin properties such as high β-O-4 linkage content (62/100 Ar) and molecular weights (6805 g/mol of M_w and 4343 g/mol of M_n) along with enhanced molecular weight distribution ($Đ$: 1.56).

Yin et al. proposed a γ-valerolactone (GVL) and p-TsOH aqueous solution (p-TsOH aq) co-solvent pretreatment for the depolymerization of moso bamboo.[65] The high efficiency and specificity of the pretreatment were confirmed with its over 98% separation of hemicellulose and lignin and up to 773 mg/g of glucose by enzymatic hydrolysis of the pretreated biomass. The separated lignin showcased high purity (>97%) with 4.88, 3710, and 760 g/mol of $Đ$, M_w, and M_n, respectively. Even if the authors used p-TsOH, they only discussed GVL and water aggregation around lignin. Because of the low concentrations (7.5%) of p-TsOH, it might be applied as a catalyst.

Wei et al. also developed a recyclable pretreatment process for herb residues using an ionic liquid (IL) assisted by *p*-TsOH.[113] The addition of 1% *p*-TsOH significantly enhanced the performance of IL pretreatment, resulting in a remarkable cellulose recovery of 96% and a high saccharification yield of 99%. By optimizing the conditions to 130 °C, 2 h, 1.0% *p*-TsOH, 79% IL, and 20% H_2O, they achieved excellent yield, purity, and thermal stability of the byproduct lignin. However, as we discussed earlier, the concentration of *p*-TsOH in this study was below its MHC, so it might work only as a catalyst without hydrotropic effect.

Zhai et al. developed a three-constituent deep eutectic solvent (3c-DES) composed of *p*-TsOH (acidic hydrogen bond acceptor), ethylene glycol (neutral hydrogen bon donor), and another hydrogen bond acceptor (chlorin chloride, tetrapropylammonium chloride or tetrabutylammonium chloride) for fractionating bamboo.[140] The optimized 3c-DES formulation achieved remarkable results, removing over 93% xylan and 90% lignin while retaining 87% cellulose in bamboo at 100 °C within 10 min. This pretreatment effectively deconstructed the recalcitrant cell walls, resulting in an impressive enzymatic hydrolysis yield of 90%, nearly four times higher than untreated bamboo. The extracted lignin exhibited high purity (95%), with 3658 g/mol of Mw and 2.77 of Đ. However, like other protonic acid catalytic processes, the Cα position of β-O-4 linkage was protonated and caused condensation with the electron-rich aromatics by this acidic DES. The authors recycled this 3c-DES three times and reported comparable delignification efficiency but decreased due to the contaminants like degraded compounds in the recycled DES. Even though the concentration of *p*-TsOH is higher than its MHC (11.5 wt%), due to the unique structure of DES composed of HBD and HBA, its hydrotropic effect was not clearly discussed or proven.

Table 5. Biomass fractionation performance and product properties by hydrotrope with other processing approaches.

Pretreatments & solvents	Biomass	Pretreatment condition	Fractionation Performance	Product Properties	Ref.
Mixed solvents (*p*-TsOH/ethanol)	Poplar sawdust	• 85 °C; 5 h	• Cellulose loss : 1% • Hemicellulose removal : 50% • Delignification : 84%	• M_w: 2070 –2630 g/mol • Đ: 1.94–2.46 • S/G ratio : 1.82–2.71	137
Mixed solvents (*p*-TsOH and methanol)	Bamboo stem	• 110 °C; 30 min	• Cellulose loss : 13% • Hemicellulose removal : 90% • Delignification : 88%	• Enzymatic hydrolysis yield of glucan: 89% • Methyl xyloside yield: 10% • Lignin with Đ (1.80) and high purity (>94%)	138
Mannitol (MT)-assisted *p*-TsOH /pentanol pretreatment	Poplar	• 120 °C; 40 min	• Delignification : 90%	• Enzymatic hydrolysis yield of glucan: 95% • Furfural yield: 84% • Lignin M_w & Đ : 6805 g/mol & 1.56 • β-O-4 bond of lignin: 62/100 Ar	139
γ-valerolactone (GVL)/ *p*-TsOH	Moso bamboo	• 130 °C; 60 min	• Cellulose loss : 8% • Hemicellulose removal : 99% • Delignification : 98%	• Enzymatic hydrolysis yield of glucan: 773 mg/g of glucose • M_w: 3710 g/mol • Đ: 4.88	65
Mixed solvents ([Bmim]Cl-TsOH solvent)	Herb residues biomass	• 130 °C; 120 min	• Cellulose loss : 4% • Hemicellulose removal : 79% • Delignification : 80%	• Enzymatic hydrolysis yield of glucan and xylan: 99%	113

| Three HBAs (ChCl, N$_4$Cl and N$_3$Cl), a neutral HBD (EG), and an acidic HBA (*p*-TsOH) | Bamboo wood | • 100 °C; 10 min | • Cellulose loss : 13%
 • Hemicellulose removal : 93%
 • Delignification : 90% | • Enzymatic hydrolysis yield of glucan: 90% (ChCl-EG-TsOH)
 • M$_w$ (3658 g/mol and *Đ*: 2.77) (ChCl-EG-TsOH) | 140 |

6. Challenges and future perspectives

Acid hydrotropic phenomena for plant biomass fractionation have shown great performance via their unique lignin dissolution capability. Most hydrotropes resulted in significant delignification, which led to great enzymatic cellulose saccharification of the fractionated cellulosic solids, even with mild processing. However, the acidic nature of the applied hydrotropes can cause repolymerization reactions.[20, 40, 49] The esterification of lignin in MAHF can protect cleaved lignin from repolymerization[6] to result in light-colored and reactive lignin favorable for producing lignin aromatics through catalytic depolymerization and also induced/enhanced electrostatic repulsive interaction between lignin and cellulase to significantly reduce nonproductive cellulase binding to lignin and therefore enhanced cellulose enzymatic saccharification.[40] However, more studies about lignin transformation with other hydrotropes are necessary.

For the successful commercialization of the hydrotropic solvent process in biomass utilization, the solvent recyclability, techno-economic feasibility and environmental impacts of this solvent system are also important. The threshold of solvent recovery can be determined based on the overall productivity as well as energy and chemical inputs for the overall process. Due to the limited penetration efficiency of organic acid into lignin structure at mild reaction

conditions,[128] high concentration of hydrotrope is required to achieve high delignification.[21, 53] Unfortunately, this high concentration leads to significant acid usage and its recovery cost, as well as equipment corrosion when using strong acid hydrotropes. Only a few studies investigated the reusability of hydrotropes,[21, 49] and the authors used energy-intensive rotary evaporation for laboratory recovery. To address the challenge of their recovery, crystallization technology was proposed by cooling the re-concentrated acid solution after lignin precipitation because of its low water solubility.[21, 52] However, the crystallization of hydrotrope was not verified with actual experiments.

The recovery of the target intermediates and products is as important as their conversion efficiencies. Many studies conducted lignin recovery from hydrolysates by precipitation via dilution below the MHC of hydrotropes. However, this precipitation method is costly because of its excessive water use and dilution of hemicelluloses in the hydrolysates. Membrane separation could be a solution, but conventional membranes have limited stability at extreme pH; therefore, a certain level of dilution is still needed. Moreover, the separation efficiency, quality and composition of the recovered hemicelluloses or hemicellulose-derived intermediates are not well studied. Besides, resin adsorption of dissolved lignin can be another option for hydrotrope recycling, but the energy demand in evaporation and cooling in the crystallization step needs to be carefully investigated.

In batch processes, the solubilized components such as hemicelluloses and lignin are readily converted further, causing degradation or condensation, even though the hydrotropic effect can reduce these side reactions. Instead of applying a new solvent, modifying the processing method with hydrotropes can be another solution for preventing the undesired transformation of biomass components. For example, a flow-through process can prevent side reactions like lignin

condensation and degradation of hemicellulose into furans by minimizing their retention time in the reactor.[6, 124, 141] The short reaction time of hydrotropic fractionation is very suitable for using a flow-through process. Microwave-assisted hydrotropes also fractionated biomass effectively without the formation of fermentation inhibitors, implying fewer side reactions occurred.[135] It implies that reactor/process design can systematically improve the hydrotropic solvent effectiveness further.

As discussed earlier, the characteristics, including amphiphilicity and acidity of hydrotropic solvents, vary depending on their structures; however, only a few hydrotropes have been studied in biomass fractionation. Based on the target products from biomass as well as environmental and economic needs, new hydrotropic solvents should be developed. In addition, a deeper elucidation of hydrotropic phenomena with biomass components is necessary to design a better solvent system. For instance, Martins et al. reported hydrotrope aggregation before the introduction of solute is negative on its hydrotropic effect, so solute-induced clustering would be a major hydrotropic mechanism.[142] Due to the heterogeneity and complexity of lignocellulosic biomass, the effects of hydrotropes on biomass vary depending on biomass species, growing environment, and others. This feedstock variability makes a comprehensive understanding of hydrotropes in biomass processing difficult. Therefore, further mechanistic study of hydrotropes with individual biomass components would be beneficial to overcome the technical challenges related to feedstock variability. This information will give a clue on how to design hydrotropes and optimize the processing conditions as well as lignin and hemicellulose recovery and the solvent recycling steps, which directly affect the economic feasibility of this strategy. Lastly, the sustainability of hydrotropic solvents and their process for biomass utilization via cradle-to-grave life cycle assessment is required to achieve their eco-manufacturing applications.

Conflicts of interest

There are no conflicts to declare.

Acknowledgements

References

1.   T. Raj, K. Chandrasekhar, A. N. Kumar and S.-H. Kim, *Renew. sustain. energy rev.*, 2022, **158**, 112130.

2.   F. H. Isikgor and C. R. Becer, *Polym. Chem.*, 2015, **6**, 4497-4559.

3.   C. Xu, R. A. D. Arancon, J. Labidi and R. Luque, *Chem. Soc. Rev.*, 2014, **43**, 7485-7500.

4.   Q. Zhai, S. Han, C.-Y. Hse, J. Jiang and J. Xu, *Ind. Crops Prod.*, 2022, **177**, 114435.

5.   Y. Song, R. P. Chandra, X. Zhang, T. Tan and J. N. Saddler, *Sustain. Energy Fuels*, 2019, **3**, 1329-1337.

6.   J. Y. Zhu, L. H. Chen and C. Cai, *ChemSusChem*, 2021, **14**, 3031-3046.

7.   H. Chen, B. Jiang, W. Wu and Y. Jin, *Int. J. Biol. Macromol.*, 2020, **151**, 861-869.

8.   B. Liu, L. Liu, B. Deng, C. Huang, J. Zhu, L. Liang, X. He, Y. Wei, C. Qin, C. Liang, L. Shijie and Y. Shuangquan, *Int. J. Biol. Macromol.*, 2022, **222**, 1400-1413.

9.   J. Zhu and X. Pan, *Renew. sustain. energy rev.*, 2022, **164**, 112583.

10. S. C. Rabelo, P. Y. S. Nakasu, E. Scopel, M. F. Araújo, L. H. Cardoso and A. C. da Costa, *Bioresour. Technol.*, 2022, **369**, 128331.

11. J. B. Ocreto, W.-H. Chen, A. P. Rollon, H. C. Ong, A. Pétrissans, M. Pétrissans and M. D. G. De Luna, *J. Chem. Eng.*, 2022, **445**, 136733.

12. X. Meng, Y. Wang, A. J. Conte, S. Zhang, J. Ryu, J. J. Wie, Y. Pu, B. H. Davison, C. G. Yoo and A. J. Ragauskas, *Bioresour. Technol.*, 2022, **368**, 128280.

13. R. Li, Y. Zheng, X. Zhao, Q. Yong, X. Meng, A. J. Ragauskas and C. Huang, *Green Chem.*, 2023, **25**, 2505-2523.

14. C. M. Cai, T. Zhang, R. Kumar and C. E. Wyman, *Green Chem.*, 2013, **15**, 3140-3145.

15. M. Chen, F. Malaret, A. E. Firth, P. Verdía, A. R. Abouelela, Y. Chen and J. P. Hallett, *Green Chem.*, 2020, **22**, 5161-5178.

16. J. Shi, J. M. Gladden, N. Sathitsuksanoh, P. Kambam, L. Sandoval, D. Mitra, S. Zhang, A. George, S. W. Singer, B. A. Simmons and S. Singh, *Green Chem.*, 2013, **15**, 2579-2589.

17. J. S. Luterbacher, J. M. Rand, D. M. Alonso, J. Han, J. T. Youngquist, C. T. Maravelias, B. F. Pfleger and J. A. Dumesic, *Science*, 2014, **343**, 277-280.

18. J. T. Gorke, F. Srienc and R. J. Kazlauskas, *Chem. Commun.*, 2008, **10**, 1235-1237.

19. X. Tang, M. Zuo, Z. Li, H. Liu, C. Xiong, X. Zeng, Y. Sun, L. Hu, S. Liu and T. Lei, *ChemSusChem*, 2017, **10**, 2696-2706.

20. D. He, Y. Wang, C. G. Yoo, Q.-J. Chen and Q. Yang, *Green Chem.*, 2020, **22**, 5414-5422.

21. L. Chen, J. Dou, Q. Ma, N. Li, R. Wu, H. Bian, D. J. Yelle, T. Vuorinen, S. Fu, X. Pan and J. Y. Zhu, *Sci. Adv.*, 2017, **3**, e1701735.

22. L. Soh and M. J. Eckelman, *ACS Sustain. Chem. Eng.*, 2016, **4**, 5821-5837.

23. E. K. New, S. K. Tnah, K. S. Voon, K. J. Yong, A. Procentese, K. P. Y. Shak, W. Subramonian, C. K. Cheng and T. Y. Wu, *J. Environ. Manage.*, 2022, **307**, 114385.

24. M. N. Borand and F. Karaosmanoğlu, *J. Renew. Sustain. Energy*, 2018, **10**, 033104.

25. B. Kudłak, K. Owczarek and J. Namieśnik, *Environ. Sci. Pollut. Res.*, 2015, **22**, 11975-11992.

26. S. Rezania, B. Oryani, J. Cho, A. Talaiekhozani, F. Sabbagh, B. Hashemi, P. F. Rupani and A. A. Mohammadi, *Energy*, 2020, **199**, 117457.

27. E. L. de Faria, S. V. Shabudin, A. F. M. Claúdio, M. Válega, F. M. Domingues, C. S. Freire, A. J. Silvestre and M. G. Freire, *ACS Sustain. Chem. Eng.*, 2017, **5**, 7344-7351.

28. A. F. M. Cláudio, M. C. Neves, K. Shimizu, J. N. C. Lopes, M. G. Freire and J. A. Coutinho, *Green Chem.*, 2015, **17**, 3948-3963.

29. K. B. Ansari and V. G. Gaikar, *Chem. Eng. Sci.*, 2014, **115**, 157-166.

30. L. P. Devendra and A. Pandey, *Renew. Energy*, 2016, **98**, 2-8.

31. H. Mou and S. Wu, *Cellulose*, 2017, **24**, 85-94.

32. D. Tripathi, S. K. Raman, J. Sahoo, D. K. Sharma and A. K. Rai, *Biointerface Res. Appl. Chem.*, 2023, **13**, 91.

33. A. Perianes-Rodriguez, L. Waltman and N. J. Van Eck, *J. Informetr.*, 2016, **10**, 1178-1195.

34. C. Neuberg, *Biochem. Z*, 1916, **76**, 107-108.

35. R. H. McKee, *US Patent 2308564*, 1943.

36. A. Procter, *Pulp Pap. Canada*, 1971, **72**, 67-74.

37. H. Mou, P. Fardim and S. Wu, in *Biomass fractionation technologies for a lignocellulosic feedstock based biorefinery*, ed. S. I. Mussatto, Elsevier, Amsterdam, Netherlands, 2016, pp. 281-313.

38. J. Olsson, M. Persson, M. Galbe, O. Wallberg and A. S. Jonsson, *Biomass Convers. Biorefin.*, 2023, **13**, 4001-4009.

39. Y. Cheng, D. M. Hall, J. Boualavong, R. J. Hickey, S. N. Lvov and C. A. Gorski, *ACS omega*, 2021, **6**, 30800-30810.

40. C. Cai, J. Li, K. Hirth, G. W. Huber, H. Lou and J. Zhu, *ChemSusChem*, 2020, **13**, 4649-4659.

41. G. Kłosowski, D. Mikulski, P. Bhagwat and S. Pillai, *Molecules*, 2022, **27**, 6097.

42. H. Fischer, E.-A. Atzpodien, M. Csato, L. Doessegger, B. Lenz, G. Schmitt and T. Singer, *J. Med. Chem.*, 2012, **55**, 126-139.

43. R. Paul, K. G. Chattaraj and S. Paul, *Langmuir*, 2021, **37**, 4745-4762.

44. C. V. Subbarao, I. K. Chakravarthy, A. Sai Bharadwaj and K. M. Prasad, *Chem. Eng. Technol.*, 2012, **35**, 225-237.

45. P. Bauduin, A. Renoncourt, A. Kopf, D. Touraud and W. Kunz, *Langmuir*, 2005, **21**, 6769-6775.

46. K. Gabov, J. Hemming and P. Fardim, *Ind. Crops Prod.*, 2017, **108**, 495-504.

47. P. J. Nelson, *Appita*, 1978.

48. D. Balasubramanian, V. Srinivas, V. Gaikar and M. Sharma, *J. Phys. Chem.*, 1989, **93**, 3865-3870.

49. C. Cai, K. Hirth, R. Gleisner, H. M. Lou, X. Q. Qiu and J. Y. Zhu, *Green Chem.*, 2020, **22**, 1605-1617.

50. C. Su, K. Hirth, Z. Liu, Y. Cao and J. Zhu, *Ind. Crops Prod.*, 2021, **159**, 113017.

51. J. Zhu, H. Zhang, N. Jiao, G. Xu and Y. Xu, *Ind. Crops Prod.*, 2022, **181**, 114853.

52. J. Zhu, L. Chen, R. Gleisner and J. Zhu, *Fuel*, 2019, **254**, 115572.

53. M. Dong, C. Wu, L. Chen, X. Zhou, W. Yang, H. Xiao, X. Ji, H. Dai, C. Hu and H. Bian, *Bioresour. Technol.*, 2021, **337**, 125379.

54. J.-Y. Yang, T.-S. Guo, Y.-H. Xu, M.-F. Li and J. Bian, *Ind. Crops Prod.*, 2023, **194**, 116269.

55. Y. Jafari, H. Amiri and K. Karimi, *Appl. Energy*, 2016, **168**, 216-225.

56. L. Yao, C. Chen, C. G. Yoo, X. Meng, M. Li, Y. Pu, A. J. Ragauskas, C. Dong and H. Yang, *ACS Sustain. Chem. Eng.*, 2018, **6**, 14767-14773.

57. L. Liang, Y.-Y. Wang, S. Bhagia, V. Sethuraman, Z. Yang, X. Meng, N. Bryant, L. Petridis, J. C. Smith and S. V. Pingali, *ACS Sustain. Chem. Eng.*, 2022, **10**, 9041-9052.

58. V. Dhapte and P. Mehta, *St. Petersburg Polytech. Univ. J.: Phys. Math.*, 2015, **1**, 424-435.

59. S. Queste, P. Bauduin, D. Touraud, W. Kunz and J.-M. Aubry, *Green Chem.*, 2006, **8**, 822-830.

60. B. P. Soares, D. O. Abranches, T. E. Sintra, A. Leal-Duaso, J. I. García, E. Pires, S. Shimizu, S. P. Pinho and J. A. Coutinho, *ACS Sustain. Chem. Eng.*, 2020, **8**, 5742-5749.

61. S. Das and S. Paul, *J. Phys. Chem. B*, 2015, **119**, 3142-3154.

62. S. Queste, Y. Michina, A. Dewilde, R. Neueder, W. Kunz and J.-M. Aubry, *Green Chem.*, 2007, **9**, 491-499.

63. D. Varade and P. Bahadur, *J. Surfactants Deterg.*, 2004, **7**, 257-261.

64. J. Byeon, J. Ko, S. Lee, D. H. Kim, S. W. Kim, D. Kim, W. Oh, S. Hong and S. J. Yoo, *ACS Energy Lett.*, 2023, **8**, 2345-2355.

65. X. Yin, T. Cai, C. Liu, C. Huang, J. Wang, J. Hu, N. Li, J. Jiang and K. Wang, *J. Chem. Eng.*, 2022, **437**, 135408.

66. L. Y. Zakharova, E. A. Vasilieva, A. B. Mirgorodskaya, S. V. Zakharov, R. V. Pavlov, N. E. Kashapova and G. A. Gaynanova, *J. Mol. Liq.*, 2022, **370**, 120923.

67. J. J. Booth, S. Abbott and S. Shimizu, *J. Phys. Chem. B*, 2012, **116**, 14915-14921.

68. F. Xiao, Z. Chen, Z. Wei and L. Tian, *Adv. Sci.*, 2020, **7**, 2001048.

69. D. O. Abranches, J. Benfica, B. P. Soares, A. Leal-Duaso, T. E. Sintra, E. Pires, S. P. Pinho, S. Shimizu and J. A. Coutinho, *Chem. Commun.*, 2020, **56**, 7143-7146.

70. S. Shimizu and N. Matubayasi, *Phys. Chem. Chem. Phys.*, 2016, **18**, 25621-25628.

71. A. A. Novikov, A. P. Semenov, A. A. Kuchierskaya, D. S. Kopitsyn, V. A. Vinokurov and M. A. Anisimov, *Langmuir*, 2019, **35**, 13480-13487.

72. A. A. Kuchierskaya, A. P. Semenov, A. R. Sayfutdinova, D. S. Kopitsyn, V. A. Vinokurov, M. A. Anisimov and A. A. Novikov, *Data Brief*, 2021, **39**, 107532.

73. M. Hahn, S. Krickl, T. Buchecker, G. Jošt, D. Touraud, P. Bauduin, A. Pfitzner, A. Klamt and W. Kunz, *Phys. Chem. Chem. Phys.*, 2019, **21**, 8054-8066.

74. A. A. Kuchierskaya, A. P. Semenov, A. R. Sayfutdinova, D. S. Kopitsyn, V. A. Vinokurov, M. A. Anisimov and A. A. Novikov, *J. Mol. Liq.*, 2021, **344**, 117683.

75. D. Mikulski and G. Kłosowski, *Sci. Rep.*, 2022, **12**, 4561.

76. J. Mehringer, E. Hofmann, D. Touraud, S. Koltzenburg, M. Kellermeier and W. Kunz, *Phys. Chem. Chem. Phys.*, 2021, **23**, 1381-1391.

77. B. Kang, H. Tang, Z. Zhao and S. Song, *ACS omega*, 2020, **5**, 6229-6239.

78. A. M. Hyde, S. L. Zultanski, J. H. Waldman, Y.-L. Zhong, M. Shevlin and F. Peng, *Org. Process Res. Dev.*, 2017, **21**, 1355-1370.

79. N. Ulmann, K. Häckl, D. Touraud and W. Kunz, *J. Colloid Interface Sci.*, 2023, **641**, 631-642.

80. S. Disale, S. Kale, G. Abraham, S. Kahandal, A. N. Sawarkar and M. B. Gawande, *Front. Chem.*, 2016, **4**, 35.

81. S. Balachandran, D. Gnana Prakash, R. Anantharaj and M. Danish John Paul, *J. Dispersion Sci.Technol.*, 2021, **42**, 1820-1829.

82. C. C. Bannan, G. Calabró, D. Y. Kyu and D. L. Mobley, *J. Chem. Theory Comput.*, 2016, **12**, 4015-4024.

83. J. A. Arnott and S. L. Planey, *Expert Opin. Drug Discov.*, 2012, **7**, 863-875.

84. E. Yara-Varón, Y. Li, M. Balcells, R. Canela-Garayoa, A.-S. Fabiano-Tixier and F. Chemat, *Molecules*, 2017, **22**, 1474.

85. J. Y. Kim, S. Kim, M. Papp, K. Park and R. Pinal, *J. Pharm. Sci.*, 2010, **99**, 3953-3965.

86. D. He, J. Zhuang, Y. Jiang, D. Xie, C. G. Yoo and Q. Yang, *ACS Sustain. Chem. Eng.*, 2021, **9**, 5364-5376.

87. V. Dordovic, Z. Tosner, M. Uchman, A. Zhigunov, M. Reza, J. Ruokolainen, G. Pramanik, P. Cígler, K. Kalikova and M. Gradzielski, *Langmuir*, 2016, **32**, 6713-6722.

88. G. Qi, L. Xiong, H. Li, Q. Huang, M. Luo, L. Tian, X. Chen, C. Huang and X. Chen, *Biomass Bioenergy*, 2019, **122**, 76-83.

89. M. S. Rishikesh, S. Harish, S. Mahendran Prasanth and D. Gnana Prakash, *Biomass Convers. Biorefin.*, 2023, **13**, 5533-5556.

90. A. D. Patel and M. A. Desai, *Tenside, Surfactants, Deterg.*, 2020, **57**, 192-202.

91. T. Buchecker, S. Krickl, R. Winkler, I. Grillo, P. Bauduin, D. Touraud, A. Pfitzner and W. Kunz, *Phys. Chem. Chem. Phys.*, 2017, **19**, 1806-1816.

92. D. Subramanian, C. T. Boughter, J. B. Klauda, B. Hammouda and M. A. Anisimov, *Faraday Discuss.*, 2013, **167**, 217-238.

93. D. O. Abranches, B. P. Soares, A. M. Ferreira, S. Shimizu, S. P. Pinho and J. A. Coutinho, *Phys. Chem. Chem. Phys.*, 2022, **24**, 7624-7634.

94. M. Hopkins Hatzopoulos, J. Eastoe, P. J. Dowding, S. E. Rogers, R. Heenan and R. Dyer, *Langmuir*, 2011, **27**, 12346-12353.

95.   C. Hansch, A. Leo, S. H. Unger, K. H. Kim, D. Nikaitani and E. J. Lien, *J. Med. Chem.*, 1973, **16**, 1207-1216.

96.   S. Lee and M. G. Barron, *PLoS One*, 2017, **12**, e0169607.

97.   M. Y. Jin, Q. Zhen, D. Xiao, G. Tao, X. Xing, P. Yu and C. Xu, *Nat. Commun.*, 2022, **13**, 3276.

98.   V. S. Kumar, C. Raja and C. Jayakumar, *Int. J. Pharm. Pharm. Sci*, 2014, **6**, 1-7.

99.   O. Pal, V. Gaikar, J. Joshi, P. Goyal and V. Aswal, *Pramana*, 2004, **63**, 357-362.

100.   C. Jayakumar and N. N. Gandhi, *J. Chem. Eng. Data*, 2010, **55**, 4362-4368.

101.   O. Diat, M. L. Klossek, D. Touraud, B. Deme, I. Grillo, W. Kunz and T. Zemb, *J. Appl. Crystallogr.*, 2013, **46**, 1665-1669.

102.   M. L. Klossek, D. Touraud, T. Zemb and W. Kunz, *ChemPhysChem*, 2012, **13**, 4116-4119.

103.   T. Zemb and W. Kunz, *Curr. Opin. Colloid Interface Sci.*, 2016, **22**, 113-119.

104.   A. D. Patel and M. A. Desai, *Rev. Chem. Eng.*, 2023, **39**, 601-630.

105.   S. Prévost, S. Krickl, S. Marčelja, W. Kunz, T. Zemb and I. Grillo, *Langmuir*, 2021, **37**, 3817-3827.

106.   A. B. Morais, C. Jayakumar and N. N. Gandhi, *Korean J. Chem. Eng.*, 2013, **30**, 925-930.

107.   A. Matero, Å. Mattsson and M. Svensson, *J. Surfactants Deterg.*, 1998, **1**, 485-489.

108.   B. Namdev, S. Venkatachalam, N. Jawahar and A. Chorsiya, *Indian J. Pharm. Educ. Res.*, 2022, **56**, 347-355.

109.   C. Marimuthu, C. Jayakumar and N. N. Gandhi, *Pet. Sci. Technol.*, 2011, **29**, 337-348.

110.   C. Jayakumar, in *Research Trends in Chemical Sciences*, ed. A. K. Acharya, AkiNik, New Delhi, India, 2019, pp. 53-75.

111. Q. Zhai, S. Yang, S. Zhao, J. Hu, Y. Lu and X. Zhang, *Int. J. Biol. Macromol.*, 2023, **253**, 126696.

112. H. Lou, J. Zhu, T. Q. Lan, H. Lai and X. Qiu, *ChemSusChem*, 2013, **6**, 919-927.

113. H.-L. Wei, J. Bu, S.-S. Zhou, M.-C. Deng and M.-J. Zhu, *J. Chem. Eng.*, 2021, **419**, 129616.

114. J. L. Cheng, K. Hirth, Q. L. Ma, J. J. Zhu, Z. J. Wang and J. Y. Zhu, *Ind. Eng. Chem. Res.*, 2019, **58**, 7063-7073.

115. P. Li, H. Ji, L. Shan, Y. Dong, Z. Long, Z. Zou and Z. Pang, *Cellulose*, 2020, **27**, 10345-10358.

116. C. Feng, J. Zhu, Y. Hou, C. Qin, W. Chen, Y. Nong, Z. Liao, C. Liang, H. Bian and S. Yao, *Bioresour. Technol.*, 2022, **348**, 126793.

117. D. E. Yüksel, L. Ballice, N. Cengiz, M. Sağlam and M. Yüksel, *Biomass Convers. Biorefin.*, 2022, **13**, 1-12.

118. W. Zhu, C. J. Houtman, J. Y. Zhu, R. Gleisner and K. F. Chen, *Process Biochem.*, 2012, **47**, 785-791.

119. Q. Ma, J. Zhu, R. Gleisner, R. Yang and J. Zhu, *ACS Sustain. Chem. Eng.*, 2018, **6**, 14480-14489.

120. Q. Duan, X. Shuai, D. Yang, X. Zhou and T. Gao, *ACS omega*, 2020, **5**, 7787-7791.

121. H. Zhou, J. Y. Zhu, X. Luo, S.-Y. Leu, X. Wu, R. Gleisner, B. S. Dien, R. E. Hector, D. Yang, X. Qiu, E. Horn and J. Negron, *Ind. Eng. Chem. Res.*, 2013, **52**, 16057-16065.

122. C. Yin, M. Wang, Q. Ma, H. Bian, H. Ren, H. Dai and J. Cheng, *Molecules*, 2021, **26**, 4123.

123. C. Feng, J. Zhu, L. Cao, L. Yan, C. Qin, C. Liang and S. Yao, *Ind. Crops Prod.*, 2022, **176**, 114374.

124. Z. J. Wang, S. Qiu, K. Hirth, J. L. Cheng, J. L. Wen, N. Li, Y. M. Fang, X. J. Pan and J. Y. Zhu, *ACS Sustain. Chem. Eng.*, 2019, **7**, 10808-10820.

125. H. Ji and P. Lv, *Green Chem.*, 2020, **22**, 1378-1387.

126. Z. Yang, R. Gleisner, D. H. Mann, J. Xu, J. Jiang and J. Zhu, *Polymers*, 2020, **12**, 2829.

127. J. Zhu, N. Jiao, J. Cheng, H. Zhang, G. Xu, Y. Xu and J. Zhu, *Renew. Energy*, 2023, **204**, 176-184.

128. H. Zeng, B. Liu, J. Li, M. Li, M. Peng, C. Qin, C. Liang, C. Huang, X. Li and S. Yao, *Bioresour. Technol.*, 2022, **351**, 126951.

129. M. Peng, J. Zhu, Y. Luo, T. Li, X. Xia, C. Qin, C. Liang, H. Bian and S. Yao, *Bioresour. Technol.*, 2022, **363**, 127879.

130. S. Ma, Y. Yan, C. He, Z. Li, X. Tang, J. Sperry, Y. Sun, L. Lin and X. Zeng, *Ind. Crops Prod.*, 2022, **180**, 114712.

131. Y. Gu, H. Bian, L. Wei and R. Wang, *Polymers*, 2019, **11**, 685.

132. Q. Lin, Y. Yan, X. Liu, B. He, X. Wang, X. Wang, C. Liu and J. Ren, *Ind. Eng. Chem. Res.*, 2020, **59**, 17429-17439.

133. Q. Yang and X. Pan, *Biotechnol. Bioeng.*, 2016, **113**, 1213-1224.

134. D. G. Prakash, K. P. Gopinath, S. M. Prasanth, S. Harish, M. Rishikesh, R. Sivaramakrishnan and A. Pugazhendhi, *Chemosphere*, 2022, **293**, 133473.

135. M. Dawid and K. Grzegorz, *Appl. Microbiol. Biotechnol.*, 2021, **105**, 3381-3392.

136. Y. Han, Y. Bai, J. Zhang, D. Liu and X. Zhao, *Bioresour. Bioprocess.*, 2020, **7**, 1-16.

137. D. Fan, X. Xie, C. Li, X. Liu, J. Zhong, X. Ouyang, Q. Liu and X. Qiu, *J. Agric. Food. Chem.*, 2021, **69**, 10838-10847.

138. Q. Zhai, F. Long, C.-y. Hse, F. Wang, T. F. Shupe, J. Jiang and J. Xu, *ACS Sustain. Chem. Eng.*, 2019, **7**, 19213-19224.

139. M. Madadi, M. Elsayed, F. Sun, J. Wang, K. Karimi, G. Song, M. Tabatabaei and M. Aghbashlo, *Bioresour. Technol.*, 2023, **371**, 128591.

140. Q. Zhai, F. Long, X. Jiang, C.-y. Hse, J. Jiang and J. Xu, *Ind. Crops Prod.*, 2020, **158**, 113018.

141. C. Cai, N. Li, H. Liu, J. Zhang, J. Zhu and F. Wang, *J. Chem. Eng.*, 2023, **453**, 139730.

142. A. C. Martins, J. Benfica, G. Peréz-Sanchéz, S. Shimizu, T. E. Sintra, N. Schaeffer and J. A. Coutinho, *Phys. Chem. Chem. Phys.*, 2022, **24**, 21645-21654.